

Bayesian Smoothed Quantile Regression

Bingqi Liu* Kangqiang Li† Tianxiao Pang‡

School of Mathematical Sciences, Zhejiang University, Hangzhou 310058, China

Abstract

Bayesian quantile regression (BQR) based on the asymmetric Laplace distribution (ALD) has two fundamental limitations: its posterior mean yields biased quantile estimates, and the non-differentiable check loss precludes gradient-based MCMC methods. We propose Bayesian smoothed quantile regression (BSQR), a principled reformulation that constructs a novel, continuously differentiable likelihood from a kernel-smoothed check loss, simultaneously ensuring a consistent posterior by aligning the inferential target with the smoothed objective and enabling efficient Hamiltonian Monte Carlo (HMC) sampling. Our theoretical analysis establishes posterior propriety for various priors and examines the impact of kernel choice. Simulations show BSQR reduces predictive check loss by up to 50% at extreme quantiles over ALD-based methods and improves MCMC efficiency by 20–40% in effective sample size. An application to financial risk during the COVID-19 era demonstrates superior tail risk modeling. The BSQR framework offers a theoretically grounded, computationally efficient solution to longstanding challenges in BQR, with uniform and triangular kernels emerging as highly effective.

Keywords: Bayesian inference; Hamiltonian Monte Carlo; Kernel smoothing; Posterior propriety; Quantile regression

MSC2020: Primary: 62F15, 62G08; Secondary: 62E20, 62P20

JEL Classification: Primary: C21; Secondary: C11, C14

*Corresponding author, E-mail: bqliu@zju.edu.cn (Bingqi Liu), ORCID: 0000-0003-0948-8930.

†E-mail: 11935023@zju.edu.cn (Kangqiang Li), ORCID: 0000-0002-4253-6730.

‡E-mail: txpang@zju.edu.cn (Tianxiao Pang).

Contents

1	Introduction	3
2	The Bayesian smoothed quantile regression framework	5
2.1	Motivation: The challenge of non-smoothness in Bayesian quantile inference	5
2.2	Technical foundation: Kernel smoothing of the check loss	7
2.3	The BSQR likelihood and posterior	8
3	Asymptotic posterior consistency	9
4	Posterior propriety under various prior specifications	11
4.1	Propriety with an improper uniform prior for β	11
4.2	Propriety with proper priors for β	13
5	Theoretical analysis of kernel selection in BSQR	15
5.1	Implications of kernel selection	15
5.2	Kernel effects on posterior concentration	16
6	Bayesian inference via MCMC	19
6.1	Hamiltonian Monte Carlo sampling for β	20
6.1.1	Gaussian kernel	21
6.1.2	Uniform kernel	22
6.1.3	Epanechnikov kernel	22
6.1.4	Triangular kernel	23
6.2	Metropolis-Hastings sampling for θ	24
7	Simulation	26
8	Empirical analysis: Asymmetric systemic risk exposure in the post-COVID era	28
8.1	Inferential stability and economic insights from asymmetric betas	29

8.2 Predictive accuracy and sampler efficiency	29
8.3 Robustness to bandwidth selection	31
9 Discussion	33
References	34
Appendix A: Proofs	36
Appendix B: Algorithms	51
Appendix C: Derivations	53
C.1 Gaussian kernel	53
C.2 Uniform kernel	54
C.3 Epanechnikov kernel	56
C.4 Triangular kernel	58
Appendix D: Simulation results	60

1 Introduction

Quantile regression (QR), pioneered by [Koenker and Bassett \(1978\)](#), provides a comprehensive framework for modeling the conditional distribution of a response variable. Unlike ordinary least squares (OLS), which targets only the conditional mean, QR offers a robust characterization of distributional heterogeneity, leading to its adoption across diverse fields, including economics ([Chernozhukov, Fernández-Val, & Melly, 2013](#)) and public health ([Koenker, 2005](#)). In the Bayesian paradigm, QR enables coherent uncertainty quantification and flexible model construction. A key breakthrough for Bayesian quantile regression (BQR) was the link between check loss minimization and maximizing a likelihood based on the asymmetric Laplace distribution (ALD) ([Yu & Moyeed, 2001](#)). Combined with the scale-mixture-of-normals representation for efficient Gibbs sampling

(Kozumi & Kobayashi, 2011), this connection spurred a rich literature, including advances in variable selection (Alhamzawi & Ali, 2018; Li, Xi, & Lin, 2010) and methods for complex data structures (Reich, Fuentes, & Dunson, 2011).

However, the standard ALD-based BQR framework has two fundamental limitations. First, its inferential target is misaligned: the posterior mean—the standard Bayesian point estimate—is a biased estimator of the true conditional quantile and fails to minimize the expected check loss (Sriram et al., 2013; Yang et al., 2016). This is a critical flaw, as the check loss is the unique proper scoring rule for quantile forecasts (Gneiting, 2011). Second, the non-differentiable check loss function, $\rho_\tau(u) = u(\tau - \mathbb{I}(u < 0))$, precludes modern gradient-based samplers like Hamiltonian Monte Carlo (HMC) and the No-U-Turn sampler (NUTS) (Hoffman & Gelman, 2014; Neal, 2011). These algorithms offer dramatic efficiency gains, especially in high dimensions (Betancourt, 2017), leaving practitioners limited to less efficient Gibbs samplers prone to slow convergence.

While smoothing the check loss has precedent in frequentist QR (Fernandes et al., 2021; Horowitz, 1998), our work moves beyond using it as a mere computational device. We leverage smoothing to construct a *new, fully coherent Bayesian likelihood* directly from a smoothed loss function. This principled construction redefines the inferential target to align with the smoothed objective, a novel approach in the BQR literature. To our knowledge, this represents the first systematic development of such a framework, forming a core contribution of this work.

Building on this, we introduce Bayesian smoothed quantile regression (BSQR). Our framework replaces the non-smooth check loss with a kernel-smoothed version,

$$L_h(\cdot; \tau) = \int_{-\infty}^{\infty} \rho_\tau(\cdot - v) K_h(v) dv = (\rho_\tau * K_h)(\cdot),$$

from which we define a novel likelihood whose density is proportional to the exponentiated negative smoothed loss,

$$f_{\text{SQR}}(\cdot) \propto \exp(-\theta L_h(\cdot; \tau)),$$

where $\theta > 0$ is a scale parameter. This paper’s contributions are fivefold: we (1) establish asymptotic

posterior consistency for BSQR, resolving the inferential bias of the ALD approach; (2) enable efficient gradient-based sampling via HMC and NUTS; (3) derive conditions for posterior propriety and show convergence to standard BQR as the smoothing bandwidth $h \rightarrow 0$; (4) analyze the impact of kernel selection on inference; and (5) demonstrate superior predictive accuracy and computational efficiency through extensive simulations and an empirical application, slashing out-of-sample prediction errors by up to 50% and boosting sampler efficiency by over 80%. The complete source code is publicly available for reproducibility.¹

The remainder of this paper is organized as follows. Section 2 presents the BSQR model. Sections 3, 4, and 5 establish its core theoretical properties. Section 6 details the computational framework. Sections 7 and 8 present simulation evidence and an empirical application. Section 9 concludes. All proofs, algorithms, technical derivations, and the simulation results tables are provided in the appendices.

2 The Bayesian smoothed quantile regression framework

This section develops the BSQR framework. We first review the fundamental limitations of standard BQR to motivate our approach, then lay out the technical foundations of loss smoothing, and finally construct our principled Bayesian model upon this foundation.

2.1 Motivation: The challenge of non-smoothness in Bayesian inference

The linear QR model posits that for i.i.d. observations (y_i, \mathbf{x}_i) from a joint distribution (Y, \mathbf{X}) , the τ -th conditional quantile of the response Y is a linear function of covariates for a given $\tau \in (0, 1)$:

$$Q_Y(\tau | \mathbf{x}_i) = \mathbf{x}_i^\top \boldsymbol{\beta}(\tau), \quad i = 1, \dots, n, \quad (1)$$

¹The replication package is available at <https://github.com/BeauquinLau/BSQR>.

where $Q_Y(\tau \mid \mathbf{x}_i) := \inf\{q : F_{Y|\mathbf{X}}(q \mid \mathbf{x}_i) \geq \tau\}$ is defined by the conditional cumulative distribution function (CDF) $F_{Y|\mathbf{X}}$, $\mathbf{x}_i \in \mathbb{R}^d$ is a covariate vector including an intercept, and $\beta(\tau) \in \mathbb{R}^d$ is the coefficient vector. This implies the error term $\varepsilon_i := y_i - \mathbf{x}_i^\top \beta(\tau)$ has a zero τ -th conditional quantile, $Q_\varepsilon(\tau \mid \mathbf{x}_i) = 0$. The standard assumption of independence between ε_i and \mathbf{x}_i simplifies this to the unconditional requirement $F_\varepsilon(0) = \tau$.

The population coefficient vector $\beta(\tau)$ is the minimizer of the expected check loss (Koenker & Bassett, 1978):

$$R(\mathbf{b}; \tau) := \mathbb{E} [\rho_\tau(\zeta)] = \int_{-\infty}^{\infty} \rho_\tau(e) dF_\zeta(e), \quad (2)$$

where $\zeta := Y - \mathbf{X}^\top \mathbf{b}$ is the population-level residual for a candidate vector \mathbf{b} , F_ζ is its CDF, and $\rho_\tau(e) = e(\tau - \mathbb{I}(e < 0))$ is the non-differentiable ‘pinball’ loss. Correspondingly, the sample estimator $\hat{\beta}(\tau)$ minimizes the empirical risk:

$$\hat{R}(\mathbf{b}; \tau) := \frac{1}{n} \sum_{i=1}^n \rho_\tau(e_i(\mathbf{b})), \quad (3)$$

where $e_i(\mathbf{b}) := y_i - \mathbf{x}_i^\top \mathbf{b}$.

The BQR paradigm connects to this objective via the ALD, whose probability density function (PDF) is $p_{\text{ALD}}(\cdot; \theta, \tau) \propto \exp(-\theta \rho_\tau(\cdot))$ (Yu & Moyeed, 2001). While this formulation ensures that its posterior mode, which we denote $\check{\beta}$, numerically coincides with the frequentist point estimator $\hat{\beta}(\tau)$, this reliance on the non-smooth check loss imposes critical limitations. First, it precludes the use of modern gradient-based samplers (e.g., HMC). Second, it creates an inferential misalignment: the posterior mean is a biased estimator of the true conditional quantile and does not minimize the expected check loss, the unique proper scoring rule for quantile forecasts (Gneiting, 2011; Sriram et al., 2013). These challenges motivate a fundamental reformulation of the Bayesian likelihood.

2.2 Technical foundation: Kernel smoothing of the check loss

The key to overcoming non-differentiability is to smooth the loss function, an idea explored in the frequentist smoothed quantile regression (SQR) literature (Fernandes et al., 2021; Horowitz, 1998). The SQR objective is formulated by replacing the discrete empirical CDF of residuals with a version smoothed by a symmetric kernel $K(\cdot)$ with bandwidth $h > 0$, where $K_h(v) = h^{-1}K(v/h)$:

$$\widehat{R}_h(\mathbf{b}; \tau, h) := \int_{-\infty}^{\infty} \rho_{\tau}(t) d\widehat{F}_h(t), \quad \text{where } \widehat{F}_h(t) = \int_{-\infty}^t \left(\frac{1}{n} \sum_{i=1}^n K_h(v - e_i(\mathbf{b})) \right) dv. \quad (4)$$

This integral can be re-expressed in a more tractable form. Expanding the definition of $d\widehat{F}_h(t)$ yields:

$$\widehat{R}_h(\mathbf{b}; \tau, h) = \frac{1}{n} \sum_{i=1}^n \int_{-\infty}^{\infty} \rho_{\tau}(t) K_h(t - e_i(\mathbf{b})) dt = \frac{1}{n} \sum_{i=1}^n \int_{-\infty}^{\infty} \rho_{\tau}(v + e_i(\mathbf{b})) K_h(v) dv, \quad (5)$$

where the second equality follows from a change of variables. This motivates defining a *smoothed check loss function*:

$$\begin{aligned} L_h(e; \tau) &:= \int_{-\infty}^{\infty} \rho_{\tau}(v + e) K_h(v) dv = \int_{-\infty}^{\infty} \rho_{\tau}(w) K_h(w - e) dw \\ &= \int_{-\infty}^{\infty} \rho_{\tau}(w) K_h(e - w) dw = (\rho_{\tau} * K_h)(e). \end{aligned} \quad (6)$$

As the convolution of the check loss and the kernel, this function allows the SQR objective to be written compactly as an average smoothed loss, whose minimizer is the SQR estimator $\hat{\beta}_h(\tau)$:

$$\widehat{R}_h(\mathbf{b}; \tau, h) = \frac{1}{n} \sum_{i=1}^n L_h(e_i(\mathbf{b}); \tau), \quad \text{where } \hat{\beta}_h(\tau) := \arg \min_{\mathbf{b} \in \mathbb{R}^d} \widehat{R}_h(\mathbf{b}; \tau, h). \quad (7)$$

A key advantage of this formulation is differentiability. The derivative of the smoothed loss,

$\Psi_h(e; \tau)$, is the convolution of the check loss subderivative $\psi_\tau(e) = \tau - \mathbb{I}(e < 0)$ ² with the kernel:

$$\Psi_h(e; \tau) := \frac{\partial L_h(e; \tau)}{\partial e} = (\psi_\tau * K_h)(e) = \int_{-\infty}^{\infty} \psi_\tau(e - v) K_h(v) dv. \quad (8)$$

This simplifies to a clean form using the kernel's CDF, $F_K(\cdot)$, as shown in Eq. (16):

$$\Psi_h(e; \tau) = F_K\left(\frac{e}{h}\right) - (1 - \tau). \quad (9)$$

This analytical gradient is fundamental for efficient HMC-based Bayesian inference, as detailed in Section 6.

2.3 The BSQR likelihood and posterior

Since the ALD-based likelihood does not target the SQR estimator $\hat{\beta}_h(\tau)$ due to $L_h(e; \tau) \neq \rho_\tau(e)$, achieving both computational efficiency and inferential coherence requires a new likelihood. The core of our BSQR model is a novel error distribution, f_{SQR} , defined from first principles with negative log-density proportional to the smoothed check loss:

$$f_{\text{SQR}}(\varepsilon; \theta, \tau, h) = \frac{1}{Z(\theta, \tau, h)} \exp(-\theta L_h(\varepsilon; \tau)),$$

where $\theta > 0$ is a scale parameter and $Z(\theta, \tau, h)$ is the normalizing constant required for f_{SQR} to be a valid PDF:

$$Z(\theta, \tau, h) := \int_{-\infty}^{\infty} \exp(-\theta L_h(u; \tau)) du. \quad (10)$$

²Strictly speaking, $\psi_\tau(e) = \tau - \mathbb{I}(e < 0)$ is a subderivative, as $\rho_\tau(e)$ is non-differentiable at $e = 0$ due to the discontinuity in ψ_τ . However, this non-differentiability does not affect the subsequent smoothing and computation, as the convolution with a sufficiently smooth kernel K_h yields a differentiable Ψ_h .

³The interchange of differentiation and integration is justified by the dominated convergence theorem. The partial derivative of the integrand with respect to e , namely $\psi_\tau(e - v) K_h(v)$, is bounded in absolute value by $\max(\tau, 1 - \tau) K_h(v)$. This dominating function is integrable over $v \in \mathbb{R}$ since K_h is a probability density, thus satisfying the conditions for the theorem.

For an observed dataset $\mathbf{y} = (y_1, \dots, y_n)^\top$ and $\mathcal{X} = (\mathbf{x}_1^\top, \dots, \mathbf{x}_n^\top)^\top$, the joint likelihood for parameters β and θ is:

$$L(\mathbf{y} | \mathcal{X}, \beta, \theta; \tau, h) = \prod_{i=1}^n f_{\text{SQR}}(e_i(\beta); \theta, \tau, h) = (Z(\theta, \tau, h))^{-n} \exp\left(-\theta \sum_{i=1}^n L_h(e_i(\beta); \tau)\right). \quad (11)$$

The log-likelihood is thus:

$$\ell(\mathbf{y} | \mathcal{X}, \beta, \theta; \tau, h) = -n \log Z(\theta, \tau, h) - \theta \sum_{i=1}^n L_h(e_i(\beta); \tau). \quad (12)$$

By construction, maximizing this with respect to β is equivalent to minimizing the SQR objective (Eq. (7)), establishing a principled link between our Bayesian model and the SQR estimator. With independent priors $\pi(\beta, \theta) = \pi(\beta)\pi(\theta)$, the posterior is:

$$\pi(\beta, \theta | \mathbf{y}, \mathcal{X}; \tau, h) \propto (Z(\theta, \tau, h))^{-n} \exp\left(-\theta \sum_{i=1}^n L_h(e_i(\beta); \tau)\right) \pi(\beta)\pi(\theta).$$

This formulation not only enables efficient gradient-based sampling (Section 6), but its critical theoretical virtue is large-sample consistency. As established in Section 3, our posterior rectifies the known inferential bias of standard BQR by consistently targeting the true quantile parameters.

3 Asymptotic posterior consistency

Posterior consistency—the concentration of the posterior distribution around the true parameter as the sample size increases—is a foundational property for any Bayesian model. This property is particularly critical for BSQR because the posterior mean from the standard ALD-based BQR is known to be inconsistent (Sriram et al., 2013). This section formally establishes that the BSQR posterior is consistent, providing a theoretical guarantee that our estimator targets the correct parameter and resolves the inferential bias of the standard approach.

Assumption 1 (Regularity conditions for consistency). *Let the true data generating process be*

governed by a linear conditional quantile model, such that $Q_Y(\tau \mid \mathbf{x}_i) = \mathbf{x}_i^\top \beta_0(\tau)$, where $\beta_0(\tau)$ is the true parameter vector. Define the error term as $\varepsilon_{0i} = y_i - \mathbf{x}_i^\top \beta_0(\tau)$. By construction, the τ -th conditional quantile of ε_{0i} given \mathbf{x}_i is zero, which implies that $F_{\varepsilon_0}(0) = \tau$. This defines the error structure implied by the model in Eq. (1) under the true parameter $\beta_0(\tau)$. The following conditions are assumed to hold:

(C1) Parameter Space: The parameter space \mathcal{B} for $\beta(\tau)$ is a compact subset of \mathbb{R}^d , with the true parameter $\beta_0(\tau)$ in its interior.

(C2) Error Distribution: The error term ε_{0i} satisfies the following:

- (a) The CDF $F_{\varepsilon_0}(\cdot)$ is at least twice continuously differentiable in a neighborhood of 0, with a PDF $f_{\varepsilon_0}(\cdot) = F'_{\varepsilon_0}(\cdot)$ that is positive at 0, i.e., $f_{\varepsilon_0}(0) > 0$.
- (b) The first moment of the error is finite, i.e., $\mathbb{E}[|\varepsilon_{0i}|] < \infty$.

(C3) Covariates: The covariate vectors \mathbf{x}_i are i.i.d. and uniformly bounded. The sample second moment matrix converges in probability to a positive definite matrix Σ_X as $n \rightarrow \infty$, i.e., $n^{-1} \sum_{i=1}^n \mathbf{x}_i \mathbf{x}_i^\top \xrightarrow{P} \Sigma_X$.

(C4) Kernel Properties: The kernel function $K(\cdot)$ is a symmetric, bounded PDF satisfying $\int_{-\infty}^{\infty} u K(u) \, du = 0$ and $\int_{-\infty}^{\infty} u^2 K(u) \, du < \infty$.

(C5) Prior Distribution: The prior distribution $\pi(\beta)$ is continuous and assigns positive probability to any open neighborhood of the true parameter $\beta_0(\tau)$.

Theorem 1 (Posterior consistency of BSQR). *Under Assumption 1, the posterior distribution $\pi(\beta \mid \mathbf{y}, \mathcal{X}, \theta)$ derived from the smoothed likelihood in Eq. (11) is consistent at the true parameter value $\beta_0(\tau)$. That is, for any neighborhood U of $\beta_0(\tau)$,*

$$\int_U \pi(\beta \mid \mathbf{y}, \mathcal{X}, \theta) \, d\beta \xrightarrow{P} 1 \quad \text{as } n \rightarrow \infty,$$

where the convergence is in probability with respect to the true data generating distribution.

The proof of this theorem is provided in [Appendix A](#).

Theorem 1 provides the theoretical cornerstone for BSQR by establishing the posterior consistency that standard BQR estimators lack. The proof hinges on the *symmetrizing property* of our smoothing procedure: convolving the asymmetric check loss with a symmetric kernel yields an objective function that is asymptotically unbiased in expectation, as shown by the pivotal result that $\mathbb{E}[\Psi_h(\varepsilon_{0i}; \tau)] \rightarrow 0$. This property ensures that, in large samples, BSQR inferences — such as posterior means and credible intervals — are correctly centered on the true parameters, thereby providing a foundation for the superior out-of-sample performance observed in our simulations (Section 7), particularly at extreme quantiles where the bias of Bayesian quantile regression based on the asymmetric Laplace distribution (BQR-ALD) is most severe.

4 Posterior propriety under various prior specifications

This section investigates posterior propriety for the BSQR model under common prior choices for the regression coefficients β and the scale parameter θ . We analyze cases ranging from an improper uniform prior for β to hierarchical structures. Our analysis uses the BSQR likelihood from Eq. (11) and the shorthand $S(\beta; \tau, h) := \sum_{i=1}^n L_h(e_i(\beta); \tau)$ for the sum of smoothed losses.

4.1 Propriety with an improper uniform prior for β

We begin by analyzing posterior propriety under an improper uniform prior, $\pi(\beta) \propto 1$. This setting is particularly insightful, as it isolates the likelihood's contribution to integrability from the regularizing effects of a proper prior for β . We first establish baseline conditions for a fixed θ and then generalize to settings where θ has its own prior. Theorem 2, proved in [Appendix A](#), summarizes these results.

Theorem 2 (Propriety under improper uniform prior for β). *Let the kernel function $K(\cdot)$ be non-negative, integrate to unity, and possess a finite first absolute moment (i.e., $\int_{-\infty}^{\infty} |u|K(u) du < \infty$). Separately, assume the $n \times d$ design matrix X has full column rank d and $\pi(\beta) \propto 1$.*

(i) (Fixed θ) If the scale parameter $\theta > 0$ is fixed, then the posterior distribution of β , $\pi(\beta | \mathbf{y}, \mathbf{X}, \theta)$, is proper. Equivalently,

$$0 < \int_{\mathbb{R}^d} L(\mathbf{y} | \mathbf{X}, \beta, \theta; \tau, h) \pi(\beta) d\beta < \infty.$$

(ii) (Prior for θ) If the scale parameter θ is assigned a prior distribution $\pi(\theta)$, then for a certain constant $C_S \geq 0$, the joint posterior distribution $\pi(\beta, \theta | \mathbf{y}, \mathbf{X})$ is proper if the integral

$$\int_0^\infty \frac{\pi(\theta) e^{\theta C_S}}{(Z(\theta, \tau, h))^n \theta^d} d\theta \quad (13)$$

converges to a finite positive value. As a specific instance, if $\pi(\theta) \sim \text{Gamma}(a, b)$ with $a, b > 0$, and further assuming that $L_h(u; \tau)$ is twice continuously differentiable and attains its global minimum $L_{\min} = \min_u L_h(u; \tau)$ at a unique point u_{\min} where $L_h''(u_{\min}; \tau) > 0$, the posterior is proper if $b > C_S + nL_{\min}$ and $a + k_Z > d$, where $k_Z \geq 0$ is a constant such that $(Z(\theta, \tau, h))^{-n} = O(\theta^{k_Z})$ as $\theta \rightarrow 0$.

Remark 1. For Theorem 2(ii), the condition $b > C_S + nL_{\min}$ on the Gamma prior hyperparameter b is a significant result. Unlike standard sample-size-independent conditions, it reveals a crucial interplay between the prior specification (b), the sample size (n), and the properties of the smoothed loss function (L_{\min}). This mandates that the prior on θ must become increasingly informative (i.e., have a larger rate b) as n grows, to ensure propriety under an improper prior for β .

This requirement stems from the powerful influence of the likelihood, where n appears as an exponent in the normalizing constant term $(Z(\theta, \tau, h))^{-n}$. Its asymptotic behavior for large θ , derived via Laplace's method, is $(Z(\theta, \tau, h))^{-n} = O(\theta^{n/2} e^{n\theta L_{\min}})$. For the posterior to be integrable, the exponential decay of the Gamma prior ($e^{-b\theta}$) must dominate this exponential growth, which directly yields the condition $b > C_S + nL_{\min}$. The second condition, $a + k_Z > d$, is a more conventional safeguard against non-identifiability as $\theta \rightarrow 0$.

4.2 Propriety with proper priors for β

We now transition to proper priors for β , which can enhance regularization and simplify propriety arguments. A conventional choice, seen in many BQR methodologies (Kozumi & Kobayashi, 2011; Li et al., 2010), is a Gaussian prior, often with a large variance to create a weakly informative yet mathematically convenient specification. Theorem 3, proved in [Appendix A](#), establishes the propriety conditions under this prior.

Theorem 3 (Propriety under Gaussian prior for β). *Let the kernel function $K(\cdot)$ be non-negative and integrate to unity, and the prior for β be Gaussian, $\pi(\beta | \sigma_\beta^2) = (2\pi\sigma_\beta^2)^{-d/2} \exp\left(-\frac{\|\beta\|_2^2}{2\sigma_\beta^2}\right)$, with a fixed prior variance $\sigma_\beta^2 > 0$.*

(i) (Fixed θ) If the scale parameter $\theta > 0$ is fixed, the posterior distribution $\pi(\beta | \mathbf{y}, \mathbf{X}, \theta, \sigma_\beta^2)$ is proper. That is,

$$0 < \int_{\mathbb{R}^d} L(\mathbf{y} | \mathbf{X}, \beta, \theta; \tau, h) \pi(\beta | \sigma_\beta^2) d\beta < \infty.$$

(ii) (Prior for θ) If the scale parameter θ is assigned a proper prior distribution $\pi(\theta)$, then the joint posterior distribution $\pi(\beta, \theta | \mathbf{y}, \mathbf{X}, \sigma_\beta^2)$ is proper if the integral

$$\int_0^\infty (Z(\theta, \tau, h))^{-n} \pi(\theta) d\theta$$

converges to a finite positive value. As a specific instance, if $\pi(\theta) \sim \text{Gamma}(\theta | a_\theta, b_\theta)$ with $a_\theta > 0$ and $b_\theta > 0$, the joint posterior $\pi(\beta, \theta | \mathbf{y}, \mathbf{X}, \sigma_\beta^2, a_\theta, b_\theta)$ is proper if

$$\int_0^\infty (Z(\theta, \tau, h))^{-n} \theta^{a_\theta-1} e^{-b_\theta\theta} d\theta$$

converges to a finite positive value.

A natural extension treats the prior variance σ_β^2 as random, allowing the data to inform its scale

while increasing flexibility. Assigning σ_{β}^2 an Inverse-Gamma hyperprior, favored for its positive support and tractability, leads to the propriety result in the following corollary.

Corollary 1 (Propriety under hierarchical Gaussian prior for β). *Let the kernel $K(\cdot)$ be non-negative and integrate to unity. The prior for β is conditionally Gaussian: $\pi(\beta \mid \sigma_{\beta}^2) = (2\pi\sigma_{\beta}^2)^{-d/2} \exp\left(-\frac{\|\beta\|_2^2}{2\sigma_{\beta}^2}\right)$, and the hyperprior for σ_{β}^2 is Inverse-Gamma: $\pi(\sigma_{\beta}^2 \mid a_0, b_0) = IG(\sigma_{\beta}^2 \mid a_0, b_0)$ with $a_0 > 0$ and $b_0 > 0$.*

(i) (Fixed θ) If $\theta > 0$ is fixed, the marginal posterior distribution $\pi(\beta, \sigma_{\beta}^2 \mid \mathbf{y}, \mathbf{X}, \theta, a_0, b_0)$ is proper. Equivalently,

$$0 < \int_0^{\infty} \int_{\mathbb{R}^d} L(\mathbf{y} \mid \mathbf{X}, \beta, \theta; \tau, h) \pi(\beta \mid \sigma_{\beta}^2) \pi(\sigma_{\beta}^2 \mid a_0, b_0) d\beta d\sigma_{\beta}^2 < \infty.$$

(ii) (Prior for θ) If the scale parameter θ is assigned a proper prior distribution $\pi(\theta)$, then the joint posterior distribution $\pi(\beta, \sigma_{\beta}^2, \theta \mid \mathbf{y}, \mathbf{X}, a_0, b_0)$ is proper if the integral

$$\int_0^{\infty} (Z(\theta, \tau, h))^{-n} \pi(\theta) d\theta$$

converges to a finite positive value. As a specific instance, if $\pi(\theta) \sim \text{Gamma}(\theta \mid a_{\theta}, b_{\theta})$ with $a_{\theta} > 0$ and $b_{\theta} > 0$, the joint posterior $\pi(\beta, \sigma_{\beta}^2, \theta \mid \mathbf{y}, \mathbf{X}, a_0, b_0, a_{\theta}, b_{\theta})$ is proper if

$$\int_0^{\infty} (Z(\theta, \tau, h))^{-n} \theta^{a_{\theta}-1} e^{-b_{\theta}\theta} d\theta$$

converges to a finite positive value.

Remark 2. A proper prior for β (even if conditional) significantly simplifies propriety arguments. Since the likelihood term $\exp(-\theta S(\beta; \tau, h))$ is bounded, integrability is largely governed by the proper priors on β and its variance. Consequently, the posterior is typically proper without requiring stringent conditions on the design matrix \mathbf{X} or on relationships between prior hyperparameters and the data dimension d .

5 Theoretical analysis of kernel selection in BSQR

This section theoretically investigates how the kernel function $K(\cdot)$ shapes the BSQR posterior. We first establish that for any compact support kernel, the BSQR posterior for β is equivalent in its tail behavior to that of standard ALD-based BQR. Second, we show that more “peaked” kernels yield a more concentrated posterior. These results provide a theoretical justification for our method and a principle for kernel selection.

5.1 Implications of kernel selection

Building on Section 4, we examine how the choice of kernel $K(\cdot)$ influences the BSQR posterior. Two properties are central: (i) the behavior of the normalizing constant $Z(\theta, \tau, h)$, which governs both the likelihood and MCMC sampling of θ ; and (ii) the relationship between the BSQR and standard ALD posteriors for compact support kernels, clarifying the role of smoothing in inference on β .

Proposition 1 (Properties of $Z(\theta, \tau, h)$). *The function $Z(\theta, \tau, h)$, as defined in Eq. (10), is based on the smoothed loss $L_h(u; \tau)$ which is non-negative for all $u \in \mathbb{R}$ and not identically zero. Consequently, for fixed τ and h :*

- (i) $Z(\theta, \tau, h)$ is a strictly decreasing function of $\theta > 0$.
- (ii) $\log Z(\theta, \tau, h)$ is a convex function of $\theta > 0$.

The proof of this proposition is provided in [Appendix A](#).

Remark 3. *The convexity of $\log Z(\theta, \tau, h)$ is consequential. It implies that the θ -dependent part of the log-likelihood (Eq. (12)) is concave. If the prior $\pi(\theta)$ is also log-concave, the conditional log-posterior $\log \pi(\theta | \beta, \mathbf{y}, \mathcal{X}; \tau, h)$ is also concave. Such log-concavity is highly beneficial for MCMC sampling, as it typically ensures unimodal and well-behaved posteriors, improving sampling efficiency and convergence for θ .*

A pertinent question is how the BSQR posterior, $\pi_{\text{BSQR}}(\boldsymbol{\beta} \mid \theta, \mathbf{y}, \mathbf{X}; \tau, h)$, relates to the ALD-based posterior, $\pi_{\text{ALD}}(\boldsymbol{\beta} \mid \theta, \mathbf{y}, \mathbf{X}; \tau)$, particularly in their tail behaviors. For compact-support kernels (e.g., Uniform, Epanechnikov, Triangular, with support normalized to $[-1, 1]$), the smoothed loss $L_h(e; \tau)$ coincides with the check loss $\rho_\tau(e)$ —up to an additive constant independent of e —whenever $|e/h| > 1$, thereby localizing smoothing to residuals near zero. This motivates a formal investigation into whether the two posteriors are *equivalent* under such kernels.

We define $L_{\text{ALD}}(\mathbf{y} \mid \mathbf{X}, \boldsymbol{\beta}, \theta; \tau) \propto \exp(-\theta \sum_{i=1}^n \rho_\tau(e_i(\boldsymbol{\beta})))$, with a normalizing constant for the ALD PDF independent of $\boldsymbol{\beta}$. The corresponding posterior is $\pi_{\text{ALD}}(\boldsymbol{\beta} \mid \theta, \mathbf{y}, \mathbf{X}; \tau) \propto L_{\text{ALD}}(\mathbf{y} \mid \mathbf{X}, \boldsymbol{\beta}, \theta; \tau) \pi(\boldsymbol{\beta})$. The following theorem, proved in [Appendix A](#), establishes this equivalence.

Theorem 4 (Posterior equivalence for BSQR with compact kernels). *Assume that the kernel $K(\cdot)$ has compact support, say $[a, b]$ for finite $a < b$, is symmetric around its mean,⁴ then there exist positive constants M_1 and M_2 , independent of $\boldsymbol{\beta}$, such that for all $\boldsymbol{\beta} \in \mathbb{R}^d$:*

$$M_1 \cdot \pi_{\text{ALD}}(\boldsymbol{\beta} \mid \theta, \mathbf{y}, \mathbf{X}; \tau) \leq \pi_{\text{BSQR}}(\boldsymbol{\beta} \mid \theta, \mathbf{y}, \mathbf{X}; \tau, h) \leq M_2 \cdot \pi_{\text{ALD}}(\boldsymbol{\beta} \mid \theta, \mathbf{y}, \mathbf{X}; \tau).$$

Remark 4. *Theorem 4 establishes that, for compact support kernels, the BSQR posterior for $\boldsymbol{\beta}$ shares the same overall shape and tail behavior as the standard ALD posterior, up to a scaling factor absorbed by the normalizing constants. This theoretically justifies using BSQR as a computationally convenient alternative (e.g., for HMC) without fundamentally altering inferential conclusions about $\boldsymbol{\beta}$. This equivalence is distinct from the case of non-compact kernels (e.g., Gaussian), where the difference $L_h(e; \tau) - \rho_\tau(e)$ may be unbounded, potentially leading to different tail behaviors.*

5.2 Kernel effects on posterior concentration

Beyond tail behavior equivalence under compact-support kernels, the choice of kernel $K(\cdot)$ also influences the posterior's concentration. Intuitively, a more “peaked” kernel assigns greater weight to small residuals (scaled by h), penalizing deviations from zero more sharply and thus

⁴Specifically, $K(\cdot)$ is symmetric with respect to its mean $\mu_K := \int_{-\infty}^{\infty} u K(u) du$, meaning that $K(\mu_K + v) = K(\mu_K - v)$ for all v in the support. In the proof, we re-center the kernel to have zero mean for simplicity.

yielding a more concentrated posterior for β . We formalize this by examining the Hessian of the negative log-likelihood component of the posterior.

Let $U_L(\beta; \theta, h, K) = \theta \sum_{i=1}^n L_h(e_i(\beta); \tau)$ be the primary component of the negative log-posterior (or potential energy function) that depends on β through the sum of smoothed losses, with its argument K signifying dependence on the kernel function $K(\cdot)$. The full negative log-posterior is $U(\beta) = U_L(\beta; \theta, h, K) - \log \pi(\beta) + C_{\theta, h}$, where $C_{\theta, h}$ collects terms not dependent on β . The Hessian of $U(\beta)$ with respect to β is $\mathbf{H}(\beta) := \nabla_{\beta}^2 U(\beta) = \nabla_{\beta}^2 U_L(\beta; \theta, h, K) - \nabla_{\beta}^2 \log \pi(\beta)$.

To find the second derivative of $L_h(e; \tau)$, we differentiate the smoothed score function $\Psi_h(e; \tau)$ from Eq. (8) with respect to e :

$$\frac{\partial \Psi_h(e; \tau)}{\partial e} = \frac{\partial}{\partial e} ((\psi_{\tau} * K_h)(e)) = (\psi'_{\tau} * K_h)(e).$$

The derivative of $\psi_{\tau}(u) = \tau - \mathbb{I}(u < 0)$ is $\psi'_{\tau}(u) = \delta(u)$, where $\delta(u)$ is the Dirac delta function.⁵ Thus, we obtain

$$\frac{\partial \Psi_h(e; \tau)}{\partial e} = (\delta * K_h)(e) = \int_{-\infty}^{\infty} \delta(v) K_h(e - v) dv = K_h(e - 0) = \frac{1}{h} K\left(\frac{e}{h}\right),$$

by utilizing the sifting property of the Dirac delta function, which states $\int_{-\infty}^{\infty} f(x) \delta(x - a) dx = f(a)$.

We now derive the Hessian of $U_L(\beta; \theta, h, K)$, denoted as $\mathbf{H}_L(\beta; K)$. The first gradient of $U_L(\beta; \theta, h, K)$ with respect to β is:

$$\nabla_{\beta} U_L(\beta; \theta, h, K) = \theta \sum_{i=1}^n \frac{\partial L_h(e_i(\beta); \tau)}{\partial \beta} = \theta \sum_{i=1}^n \left(\frac{\partial L_h(e_i; \tau)}{\partial e_i} \cdot \frac{\partial e_i(\beta)}{\partial \beta} \right) = \theta \sum_{i=1}^n \Psi_h(e_i(\beta); \tau)(-x_i),$$

⁵Strictly speaking, the classical derivative of $\psi_{\tau}(u)$ does not exist at $u = 0$ due to the discontinuity. However, in the distributional sense, it is given by $\psi'_{\tau}(u) = \delta(u)$. To see this, note that $\psi_{\tau}(u) = \tau - 1 + H(u)$, where $H(u)$ is the Heaviside step function ($H(u) = 0$ for $u < 0$ and $H(u) = 1$ for $u \geq 0$). The distributional derivative of $H(u)$ is the Dirac delta $\delta(u)$, leading to $\psi'_{\tau}(u) = \delta(u)$. This does not affect the convolution, which yields a smooth second derivative.

since $\partial e_i / \partial \beta = -\mathbf{x}_i$. The Hessian is obtained by differentiating the gradient with respect to β^\top :

$$\begin{aligned}
\mathbf{H}_L(\beta; K) &= \nabla_{\beta^\top} \left(-\theta \sum_{i=1}^n \Psi_h(e_i(\beta); \tau) \mathbf{x}_i \right) = -\theta \sum_{i=1}^n \frac{\partial}{\partial \beta^\top} (\Psi_h(e_i(\beta); \tau) \mathbf{x}_i) \\
&= -\theta \sum_{i=1}^n \mathbf{x}_i \frac{\partial \Psi_h(e_i(\beta); \tau)}{\partial \beta^\top} = -\theta \sum_{i=1}^n \mathbf{x}_i \left(\frac{\partial \Psi_h(e_i; \tau)}{\partial e_i} \cdot \frac{\partial e_i(\beta)}{\partial \beta^\top} \right) \\
&= -\theta \sum_{i=1}^n \mathbf{x}_i \left(\frac{1}{h} K \left(\frac{e_i(\beta)}{h} \right) \cdot (-\mathbf{x}_i^\top) \right) = \frac{\theta}{h} \sum_{i=1}^n K \left(\frac{e_i(\beta)}{h} \right) \mathbf{x}_i \mathbf{x}_i^\top. \tag{14}
\end{aligned}$$

A larger Hessian (in the positive definite sense) at the posterior mode $\check{\beta}$ suggests a more sharply peaked posterior and, via Laplace approximation, a smaller posterior covariance.

As discussed in Section 3, the true errors $\varepsilon_{0i} = y_i - \mathbf{x}_i^\top \beta_0(\tau)$ are assumed to be independent and identically distributed following a common density $f_{\varepsilon_0}(\cdot)$, where $\beta_0(\tau)$ represents the true value of $\beta(\tau)$. Define $s_K(h) := \mathbb{E}_{\varepsilon_0 \sim f_{\varepsilon_0}} [K(\frac{\varepsilon_0}{h})]$. Let $\mathcal{H}_L(\beta_0(\tau); K) := \mathbb{E}_{\varepsilon_{0i}, \mathbf{x}_i} [\mathbf{H}_L(\beta_0(\tau); K)]$ denote the expected Hessian of the negative log-likelihood component, evaluated at the true parameter $\beta_0(\tau)$. This leads to the following theorem with the proof provided in [Appendix A](#).

Theorem 5 (Kernel peakedness and expected local curvature). *Let $K_A(v)$ and $K_B(v)$ be two distinct kernel functions that are non-negative, symmetric about zero, and share a common compact support. Assume that $s_{K_A}(h) > s_{K_B}(h)$, and that the covariates follow $\mathbf{x}_i \stackrel{i.i.d.}{\sim} P_{\mathbf{X}}$ where $P_{\mathbf{X}}$ has a positive definite covariance matrix $\Sigma_x := \mathbb{E}[\mathbf{x}_i \mathbf{x}_i^\top]$ and finite second moments. Then, for the expected Hessian:*

$$\mathcal{H}_L(\beta_0(\tau); K_A) > \mathcal{H}_L(\beta_0(\tau); K_B),$$

where $>$ denotes the strict Loewner order. Furthermore, for the sample Hessian, the corresponding inequality

$$\mathbf{H}_L(\beta_0(\tau); K_A) > \mathbf{H}_L(\beta_0(\tau); K_B)$$

holds with probability approaching 1 as $n \rightarrow \infty$.

Remark 5. *Theorem 5 establishes that a kernel K_A satisfying $s_{K_A}(h) > s_{K_B}(h)$ yields a larger expected Hessian at the true parameter. Via Laplace approximation, this increased local curvature*

implies a more concentrated posterior for β and a smaller covariance matrix (i.e., $\mathcal{H}_L(\cdot; K_A)^{-1} \leq \mathcal{H}_L(\cdot; K_B)^{-1}$), assuming the prior's Hessian is negligible.

Remark 6. The condition $s_{K_A}(h) > s_{K_B}(h)$ means that kernel K_A gives more average weight to the true scaled errors. This is likely to occur when a more “peaked” kernel K_A aligns with a concentrated error density f_{ε_0} , as more error values will fall where $K_A(v) > K_B(v)$. For instance, a Triangular kernel will likely satisfy this condition over a Uniform kernel on $[-1, 1]$ if most true errors are small, as it places more mass near zero.

Remark 7. While Theorem 5 is an asymptotic result at the true parameter $\beta_0(\tau)$, its principle extends to the posterior mode $\check{\beta}$. A more peaked kernel may yield a more concentrated posterior if it produces a consistently larger sum $\sum_{i=1}^n K(e_i(\check{\beta})/h)$ than competing kernels, based on the empirical distribution of residuals.

6 Bayesian inference via MCMC

Bayesian inference for the BSQR parameters—regression coefficients β and scale θ —is challenging, particularly when targeting uncertainty quantification. Standard BQR exploits the ALD's scale-mixture-of-normals form (Kozumi & Kobayashi, 2011; Yu & Moyeed, 2001), enabling efficient Gibbs updates. However, the smoothed loss $L_h(e; \tau)$ in our framework, while beneficial for gradient-based optimization and theoretical properties, disrupts the conditional conjugacy needed for such updates, rendering direct sampling from the joint posterior intractable.

We address this via a block-wise hybrid MCMC algorithm. The high-dimensional vector β is updated with HMC (Duane et al., 1987; Neal, 2011), a gradient-based sampler effective for complex, high-dimensional targets (Section 6.1). The scalar θ is updated with a Metropolis–Hastings (MH) step (Hastings, 1970; Metropolis et al., 1953), suitable when the likelihood's normalizing constant depends on the sampled parameter (Section 6.2). This tailored scheme enables robust and efficient exploration of the BSQR posterior landscape.

6.1 Hamiltonian Monte Carlo sampling for β

We therefore employ a hybrid MCMC approach: HMC samples $\pi(\beta \mid \theta_c, \mathbf{y}, \mathcal{X}; \tau, h)$, where θ_c is the current value of θ , and θ is subsequently updated via a Metropolis–Hastings step (Section 6.2). HMC avoids random-walk behavior by introducing auxiliary momentum variables and simulating Hamiltonian dynamics, making it efficient for complex, high-dimensional posteriors with gradient information (Duane et al., 1987; Neal, 2011).

The HMC sampler augments $\beta \in \mathbb{R}^d$ with an auxiliary momentum vector $\mathbf{p} \in \mathbb{R}^d$. The system's dynamics are governed by the Hamiltonian function:

$$H(\beta, \mathbf{p}) = U(\beta \mid \theta_c, \mathbf{y}, \mathcal{X}) + T(\mathbf{p}),$$

where the potential energy $U(\beta \mid \theta_c, \mathbf{y}, \mathcal{X})$ is the negative log-conditional posterior for β (up to a constant),

$$U(\beta \mid \theta_c, \mathbf{y}, \mathcal{X}) = \theta_c \sum_{i=1}^n L_h(e_i(\beta); \tau) - \log \pi(\beta). \quad (15)$$

The kinetic energy is $T(\mathbf{p}) = \frac{1}{2} \mathbf{p}^\top \mathbf{M}^{-1} \mathbf{p}$, with \mathbf{M} typically set to the identity matrix. The evolution over fictitious time s follows Hamilton's equations (Duane et al., 1987; Neal, 2011):

$$\begin{aligned} \frac{d\beta(s)}{ds} &= \frac{\partial H}{\partial \mathbf{p}(s)} = \mathbf{M}^{-1} \mathbf{p}(s), \\ \frac{d\mathbf{p}(s)}{ds} &= -\frac{\partial H}{\partial \beta(s)} = -\nabla_\beta U(\beta(s) \mid \theta_c, \mathbf{y}, \mathcal{X}), \end{aligned}$$

which preserve phase-space volume and are reversible. These equations are integrated using the leapfrog method. A single step of size ϵ updates (β, \mathbf{p}) via:

$$\begin{aligned} \mathbf{p}_{\text{half}} &= \mathbf{p} - \frac{\epsilon}{2} \nabla_\beta U(\beta \mid \theta_c, \mathbf{y}, \mathcal{X}), \\ \beta' &= \beta + \epsilon \mathbf{M}^{-1} \mathbf{p}_{\text{half}}, \\ \mathbf{p}' &= \mathbf{p}_{\text{half}} - \frac{\epsilon}{2} \nabla_\beta U(\beta' \mid \theta_c, \mathbf{y}, \mathcal{X}). \end{aligned}$$

The complete sampler is outlined in Algorithm 1 of [Appendix B](#). The leapfrog integrator requires the potential energy gradient, $\nabla_{\beta}U(\beta \mid \theta_c, \mathbf{y}, \mathcal{X})$. From Eq. (15), the potential energy gradient is

$$\nabla_{\beta}U(\beta \mid \theta_c, \mathbf{y}, \mathcal{X}) = \theta_c \sum_{i=1}^n \nabla_{\beta}L_h(e_i(\beta); \tau) - \nabla_{\beta} \log \pi(\beta),$$

where $\nabla_{\beta}L_h(e_i; \tau) = -\Psi_h(e_i; \tau) \mathbf{x}_i$ and Ψ_h is the smoothed score function:

$$\begin{aligned} \Psi_h(e; \tau) &= \int_{-\infty}^{\infty} (\tau - \mathbb{I}(u < 0)) \frac{1}{h} K\left(\frac{e-u}{h}\right) du \\ &= \tau \int_{-\infty}^{\infty} \frac{1}{h} K\left(\frac{e-u}{h}\right) du - \int_{-\infty}^0 \frac{1}{h} K\left(\frac{e-u}{h}\right) du \\ &= \tau \cdot 1 - \int_{e/h}^{\infty} K(z) dz = \tau - \left(1 - F_K\left(\frac{e}{h}\right)\right) \\ &= F_K\left(\frac{e}{h}\right) - (1 - \tau), \end{aligned} \tag{16}$$

where $K(\cdot)$ is the kernel density and F_K its CDF. For a Gaussian prior $\beta \sim \mathcal{N}(\beta_0, \Omega)$, the gradient is:

$$\nabla_{\beta}U(\beta \mid \theta_c, \mathbf{y}, \mathcal{X}) = -\theta_c \sum_{i=1}^n \left[F_K\left(\frac{e_i(\beta)}{h}\right) - (1 - \tau) \right] \mathbf{x}_i + \Omega^{-1}(\beta - \beta_0).$$

Evaluating $U(\beta \mid \theta_c, \mathbf{y}, \mathcal{X})$ for the HMC acceptance step requires the explicit form of $L_h(e_i; \tau)$. We now present the closed-form expressions for the smoothed score $\Psi_h(e; \tau)$ and smoothed loss $L_h(e; \tau)$ for several common kernels, with their detailed derivations provided in [Appendix C](#).

6.1.1 Gaussian kernel

The standard Gaussian kernel is $K(v) = \phi(v) = (2\pi)^{-1/2} \exp(-v^2/2)$, with CDF $F_K(u) = \Phi(u)$.

Applying Eq. (16) yields:

$$\Psi_h(e; \tau) = \Phi\left(\frac{e}{h}\right) - (1 - \tau). \tag{17}$$

The corresponding smoothed loss function $L_h(e; \tau)$, obtained by integrating $\Psi_h(e; \tau)$ and consistent with $\rho_\tau(e)$ for small h , is given by (e.g., [Horowitz, 1998](#); [Koenker, 2005](#)):

$$L_h(e; \tau) = e \left(\Phi \left(\frac{e}{h} \right) - (1 - \tau) \right) + h \phi \left(\frac{e}{h} \right).$$

6.1.2 Uniform kernel

The standard Uniform kernel is $K(v) = \frac{1}{2}$ for $v \in [-1, 1]$ and 0 otherwise. Its CDF is $F_K(u) = 0$ for $u < -1$, $F_K(u) = \frac{u+1}{2}$ for $-1 \leq u \leq 1$, and $F_K(u) = 1$ for $u > 1$. From Eq. (16), $\Psi_h(e; \tau)$ is:

$$\Psi_h(e; \tau) = \begin{cases} -(1 - \tau) & \text{if } e/h < -1, \\ \frac{e}{2h} + \tau - \frac{1}{2} & \text{if } -1 \leq e/h \leq 1, \\ \tau & \text{if } e/h > 1. \end{cases}$$

The function $L_h(e; \tau)$ is derived by integrating $\Psi_h(e; \tau)$ and imposing continuity with $\rho_\tau(e)$ for $|e/h| \geq 1$. The resulting expression is:

$$L_h(e; \tau) = \begin{cases} e(\tau - 1) & \text{if } e/h \leq -1, \\ \frac{e^2}{4h} + e \left(\tau - \frac{1}{2} \right) + \frac{h}{4} & \text{if } -1 < e/h < 1, \\ e\tau & \text{if } e/h \geq 1. \end{cases}$$

6.1.3 Epanechnikov kernel

The standard Epanechnikov kernel is $K(v) = \frac{3}{4}(1 - v^2)$ for $v \in [-1, 1]$ and 0 otherwise. Its CDF, $F_K(u)$, is 0 for $u < -1$, $\frac{3}{4}u - \frac{1}{4}u^3 + \frac{1}{2}$ for $-1 \leq u \leq 1$, and 1 for $u > 1$. This yields $\Psi_h(e; \tau)$ as:

$$\Psi_h(e; \tau) = \begin{cases} -(1 - \tau) & \text{if } e/h < -1, \\ \frac{3}{4} \frac{e}{h} - \frac{1}{4} \left(\frac{e}{h} \right)^3 + \tau - \frac{1}{2} & \text{if } -1 \leq e/h \leq 1, \\ \tau & \text{if } e/h > 1. \end{cases}$$

Integration of $\Psi_h(e; \tau)$ and matching boundary conditions with $\rho_\tau(e)$ for $|e/h| \geq 1$ leads to $L_h(e; \tau)$:

$$L_h(e; \tau) = \begin{cases} e(\tau - 1) & \text{if } e/h \leq -1, \\ \frac{3e^2}{8h} - \frac{e^4}{16h^3} + e \left(\tau - \frac{1}{2} \right) + \frac{3h}{16} & \text{if } -1 < e/h < 1, \\ e\tau & \text{if } e/h \geq 1. \end{cases}$$

6.1.4 Triangular kernel

The standard Triangular kernel is $K(v) = 1 - |v|$ for $v \in [-1, 1]$ and 0 otherwise. The CDF, $F_K(u)$, is 0 for $u < -1$; $\frac{1}{2}(1+u)^2$ for $-1 \leq u < 0$; $1 - \frac{1}{2}(1-u)^2$ for $0 \leq u \leq 1$; and 1 for $u > 1$. Consequently, $\Psi_h(e; \tau)$ is:

$$\Psi_h(e; \tau) = \begin{cases} -(1 - \tau) & \text{if } e/h < -1, \\ \frac{1}{2} \left(1 + \frac{e}{h} \right)^2 - (1 - \tau) & \text{if } -1 \leq e/h < 0, \\ 1 - \frac{1}{2} \left(1 - \frac{e}{h} \right)^2 - (1 - \tau) & \text{if } 0 \leq e/h \leq 1, \\ \tau & \text{if } e/h > 1. \end{cases}$$

The corresponding $L_h(e; \tau)$ is obtained by piecewise integration of $\Psi_h(e; \tau)$, ensuring continuity with $\rho_\tau(e)$ for $|e/h| \geq 1$ and at $e = 0$:

$$L_h(e; \tau) = \begin{cases} e(\tau - 1) & \text{if } e/h \leq -1, \\ \frac{h}{6} \left(1 + \frac{e}{h} \right)^3 - e(1 - \tau) & \text{if } -1 < e/h < 0, \\ e\tau + \frac{h}{6} \left(1 - \frac{e}{h} \right)^3 & \text{if } 0 \leq e/h < 1, \\ e\tau & \text{if } e/h \geq 1. \end{cases}$$

The HMC procedure in Algorithm 1 samples β from its conditional posterior $\pi(\beta \mid \theta_c, y, \mathcal{X})$. This forms one block of a hybrid MCMC sampler that alternates between updating β and θ (Section 6.2). A joint HMC update for (β, θ) is avoided because the gradient of the log-normalizing

constant, $\partial \log Z(\theta, \tau, h) / \partial \theta$, is intractable. The computational cost of this HMC step is dominated by the J gradient evaluations per iteration, and its key tuning parameters — the leapfrog step size ϵ , number of steps J , and mass matrix \mathbf{M} — are typically adapted using methods like the NUTS (Hoffman & Gelman, 2014), as implemented in software such as Stan and PyMC.

6.2 Metropolis-Hastings sampling for θ

Following the HMC update for β , we sample the scale parameter θ from its conditional posterior $\pi(\theta | \beta_c, \mathbf{y}, \mathbf{X}; \tau, h)$, where β_c is the most recently sampled value from Section 6.1. Applying HMC to θ is impractical: the potential energy involves the normalizing constant $Z(\theta, \tau, h)$ (defined in Eq. (10)) via the term $n \log Z(\theta, \tau, h)$. Its gradient, $\partial \log Z(\theta, \tau, h) / \partial \theta$, requires differentiating an intractable integral, lacks a closed form, and would entail costly numerical integration at each leapfrog step. We therefore employ a gradient-free Metropolis–Hastings (MH) update for θ . The target conditional posterior for θ is

$$\pi(\theta | \beta_c, \mathbf{y}, \mathbf{X}) \propto Z(\theta, \tau, h)^{-n} \exp(-\theta S(\beta_c; \tau, h)) \pi(\theta),$$

where $S(\beta_c; \tau, h) = \sum_{i=1}^n L_h(e_i(\beta_c); \tau)$. Assuming a Gamma prior, $\theta \sim \text{Gamma}(a_\theta, b_\theta)$, we define the potential energy function $U(\theta | \beta_c, \mathbf{y}, \mathbf{X})$ as the negative log-posterior $-\log \pi(\theta | \beta_c, \mathbf{y}, \mathbf{X})$, which, up to an additive constant, is given by:

$$U(\theta | \beta_c, \mathbf{y}, \mathbf{X}) = \theta S(\beta_c; \tau, h) + n \log Z(\theta, \tau, h) - \log \pi(\theta). \quad (18)$$

The MH algorithm requires a proposal distribution to generate candidate values. We employ a log-normal proposal for the scale parameter θ , drawing θ' such that $\log \theta' \sim \mathcal{N}(\log \theta_c, \sigma_{\log \theta}^2)$, where θ_c is the current state and $\sigma_{\log \theta}^2$ is a tuning variance. This proposal is symmetric on the log scale but not on the original scale, implying a non-unity Hastings ratio. The ratio, obtained by dividing the

corresponding proposal densities, is

$$\frac{q(\theta_c | \theta')}{q(\theta' | \theta_c)} = \frac{\frac{1}{\theta_c \sigma_{\log \theta} \sqrt{2\pi}} \exp\left[-\frac{(\log \theta_c - \log \theta')^2}{2\sigma_{\log \theta}^2}\right]}{\frac{1}{\theta' \sigma_{\log \theta} \sqrt{2\pi}} \exp\left[-\frac{(\log \theta' - \log \theta_c)^2}{2\sigma_{\log \theta}^2}\right]} = \frac{1/\theta_c}{1/\theta'} = \frac{\theta'}{\theta_c}. \quad (19)$$

The log acceptance ratio, $\log r$, for proposing θ^* from the current value θ_c is constructed from the potential energy and the Hastings ratio. Substituting the components from Eq. (18), the Gamma prior, and Eq. (19), the expression simplifies to:

$$\begin{aligned} \log r &= \log \pi(\theta^* | \beta_c, \mathbf{y}, \mathbf{X}) - \log \pi(\theta_c | \beta_c, \mathbf{y}, \mathbf{X}) + \log \left(\frac{q(\theta_c | \theta^*)}{q(\theta^* | \theta_c)} \right) \\ &= U(\theta_c | \beta_c, \mathbf{y}, \mathbf{X}) - U(\theta^* | \beta_c, \mathbf{y}, \mathbf{X}) + \log \theta^* - \log \theta_c \\ &= [\theta_c S(\beta_c; \tau, h) + n \log Z(\theta_c, \tau, h) - ((a_\theta - 1) \log \theta_c - b_\theta \theta_c)] \\ &\quad - [\theta^* S(\beta_c; \tau, h) + n \log Z(\theta^*, \tau, h) - ((a_\theta - 1) \log \theta^* - b_\theta \theta^*)] + (\log \theta^* - \log \theta_c) \\ &= -(\theta^* - \theta_c) S(\beta_c; \tau, h) - n(\log Z(\theta^*, \tau, h) - \log Z(\theta_c, \tau, h)) \\ &\quad + a_\theta (\log \theta^* - \log \theta_c) - b_\theta (\theta^* - \theta_c). \end{aligned}$$

This expression for $\log r$ is used in the MH sampler detailed in Algorithm 2 of Appendix B. Its implementation requires two main computations: evaluating the sum $S(\beta_c; \tau, h)$ using the kernel-specific closed-form expressions for $L_h(\cdot; \tau)$ from the preceding subsections, and numerically integrating to find the normalizing constant $Z(\theta, \tau, h)$. While the latter is computationally non-trivial, evaluating $Z(\theta, \tau, h)$ is more feasible than evaluating its gradient, justifying our choice of MH over HMC for this block. The overall MCMC procedure thus alternates between the HMC step for β (Algorithm 1) and this MH step for θ , forming an iterative block sampling (or Metropolis-within-Gibbs) scheme to draw from the joint posterior $\pi(\beta, \theta | \mathbf{y}, \mathbf{X}; \tau, h)$.

7 Simulation

We conduct a simulation study to evaluate the estimation accuracy and inferential validity of our proposed BSQR framework, using Gaussian, Uniform, Epanechnikov, and Triangular kernels (Sections 6.1.1–6.1.4). Synthetic data are generated from $y_i = \mathbf{x}_i^\top \boldsymbol{\beta}_0 + u_i$ for $i = 1, \dots, n$, with $N_{\text{train}} = 200$ and $N_{\text{test}} = 1000$ in separate training and test sets. Covariate vectors $\mathbf{x}_i \sim \mathcal{N}(\mathbf{0}, \boldsymbol{\Sigma}_X)$ have an autoregressive structure $(\boldsymbol{\Sigma}_X)_{jk} = \rho^{|j-k|}$ with $\rho = 0.5$, as in [Fan and Li \(2001\)](#). We consider two scenarios: a sparse, high-dimensional setting ($d = 20$) with $\boldsymbol{\beta}_0 = (3, 1.5, 0, 0, 2, 0, \dots, 0)^\top$, and a dense, lower-dimensional setting ($d = 8$) with $\boldsymbol{\beta}_0 = (0.85, \dots, 0.85)^\top$. Four error distributions for u_i assess robustness: (1) $\mathcal{N}(0, 1)$; (2) $t(3)$; (3) a bimodal mixture $0.2\mathcal{N}(0, 3) + 0.8\mathcal{N}(0, 4)$; and (4) heteroscedastic normal, $u_i \mid \mathbf{x}_i \sim \mathcal{N}(0, \sigma_i^2)$ with $\sigma_i = \exp(-0.25 + 0.5x_{i1})$. The last setting evaluates robustness under model misspecification, as it violates the linear conditional quantile assumption. Simulations are run for $\tau \in \{0.25, 0.5, 0.75\}$ over $M = 200$ independent replications, and all reported metrics are averaged over these runs to provide Monte Carlo estimates of their theoretical expectations.

Standard quantile regression (StdQR) is implemented via the “rq” function in the `quantreg` package, and BQR-ALD via `brms` package. BSQR is implemented in Stan using the NUTS sampler ([Hoffman & Gelman, 2014](#)), with two parallel chains of 4000 iterations each (2000 warmup), yielding 4000 post-warmup samples without thinning. The likelihood’s normalizing constant $Z(\theta, \tau, h)$ is computed at each NUTS step using a hybrid approach: an asymptotic approximation for sharply peaked integrands (e.g., large θ or specific τ and h) to avoid instability and reduce computation time, otherwise direct numerical integration via Stan’s `integrate_1d` function.

The smoothing bandwidth h governs the trade-off between fidelity to the check loss and posterior stability. A small h approximates ALD-based BQR, risking numerical issues; a large h can over-smooth, introducing bias. We select h via 5-fold cross-validation over the grid $\{0.5, 0.75, 1.0, 1.5, 2.0\}$ times Silverman’s rule, minimizing average out-of-sample check loss. A fully Bayesian treatment with a prior on h is theoretically appealing but computationally

prohibitive due to the dependence of the intractable $Z(\theta, \tau, h)$ on h . For completeness, a sensitivity analysis is presented in Section 8.3. For all Bayesian methods, priors are $\beta \sim \mathcal{N}(0, 1000I)$ and $\theta \sim \text{Gamma}(0.01, 0.01)$.

Point estimation accuracy is measured by MSE: $\|\hat{\beta} - \beta_0\|_2^2$; MAE: $\|\hat{\beta} - \beta_0\|_1/d$; WMSE: $(\hat{\beta} - \beta_0)^\top \Sigma_X (\hat{\beta} - \beta_0)$, with $\hat{\beta}$ the posterior mean. Predictive accuracy is the average check loss on the test set: $N_{\text{test}}^{-1} \sum_{i=1}^{N_{\text{test}}} \rho_\tau(y_i^{\text{test}} - x_i^{\text{test}} \hat{\beta})$. For Bayesian methods, we also report empirical coverage and average width of 95% credible intervals, computation time, and MCMC diagnostics (\hat{R}_{\max} and ESS_{\min}).

Results (see in Appendix D) validate the proposed BSQR framework, showing consistent superiority over BQR-ALD across multiple evaluation dimensions. BSQR generally excels in estimation accuracy and prediction, achieving lower MSE, MAE, and WMSE for coefficient estimates in most scenarios across error distributions, though BQR-ALD is occasionally comparable or slightly better in specific cases. Critically, BSQR resolves BQR-ALD’s predictive bias: out-of-sample check loss is reduced by 40–50% at $\tau = 0.25$ and $\tau = 0.75$, matching the frequentist StdQR benchmark, and performances are comparable at $\tau = 0.5$, confirming that smoothing restores the link between model parameters and the true conditional quantiles. For inference, BSQR delivers more reliable uncertainty quantification, with credible interval coverage often closer to 0.95; BQR-ALD’s narrower intervals frequently under-cover, while Uniform and Triangular kernels balance coverage and width effectively. Computationally, the smoothed posterior yields 20–40% higher minimum bulk ESS (e.g., 2700–3200 vs. 2100–2400 for BQR-ALD), ensuring reliable estimates, and bounded-support kernels (Uniform, Triangular, Epanechnikov) maintain near-zero divergent transitions (consistently < 2); Uniform (BSQR-U) is the fastest for large datasets — often surpassing BQR-ALD — while Triangular (BSQR-T) offers a favorable trade-off between speed, accuracy, and inference, Epanechnikov (BSQR-E) is slower with wider intervals, and Gaussian (BSQR-G) is computationally intensive and least stable. Overall, BSQR improves BQR by eliminating bias, improving computational efficiency, and favoring simple bounded-support *Uniform and Triangular kernels* for optimal trade-offs in speed, accuracy, and inference, making them the preferred choice

for applied research.

8 Empirical analysis: Asymmetric systemic risk exposure in the post-COVID era

We apply the BSQR framework to assess the asymmetric dynamics of systemic risk for a globally systemically important financial institution (G-SIFI), demonstrating its empirical utility. This section outlines methodology and results, highlighting BSQR's advantage in delivering more reliable risk quantification. Our analysis models the link between daily stock returns of JPMorgan Chase & Co. (JPM) and the S&P 500 Index (^GSPC),⁶ using daily log-returns from January 1, 2017, to January 1, 2025. Prices are converted to continuously compounded returns ($r_t = \ln(P_t/P_{t-1})$), yielding a rich time series whose summary statistics appear in Table 1. The pronounced leptokurtosis in both series strongly motivates a quantile-based approach.

Table 1. Descriptive statistics for daily log-returns.

Statistic	JPMorgan Chase (JPM)	S&P 500 Index (GSPC)
Observations	2011.0000	2011.0000
Mean	0.0006	0.0005
Std. Dev.	0.0178	0.0118
Skewness	-0.0240	-0.8614
Kurtosis	14.3309	16.2964

We specify a dynamic capital asset pricing model (CAPM) for quantile level τ :

$$Q_{\text{JPM_Return}_t}(\tau | \text{GSPC_Return}_t) = \alpha(\tau) + \beta(\tau) \cdot \text{GSPC_Return}_t,$$

where $\beta(\tau)$ measures systemic risk. To capture asymmetry, we examine the downside beta ($\beta(0.05)$), quantifying exposure during severe downturns, and the upside beta ($\beta(0.95)$), measuring participation in market rallies. Using a rolling-window estimation with a one-year window (252

⁶Data for JPM and the S&P 500 are from <https://finance.yahoo.com/quote/JPM/> and <https://finance.yahoo.com/quote/^GSPC/>.

trading days) advanced monthly (21 days), we compare BSQR (Uniform and Triangular kernels) with the BQR-ALD benchmark across inferential stability, predictive accuracy, and sampler efficiency.

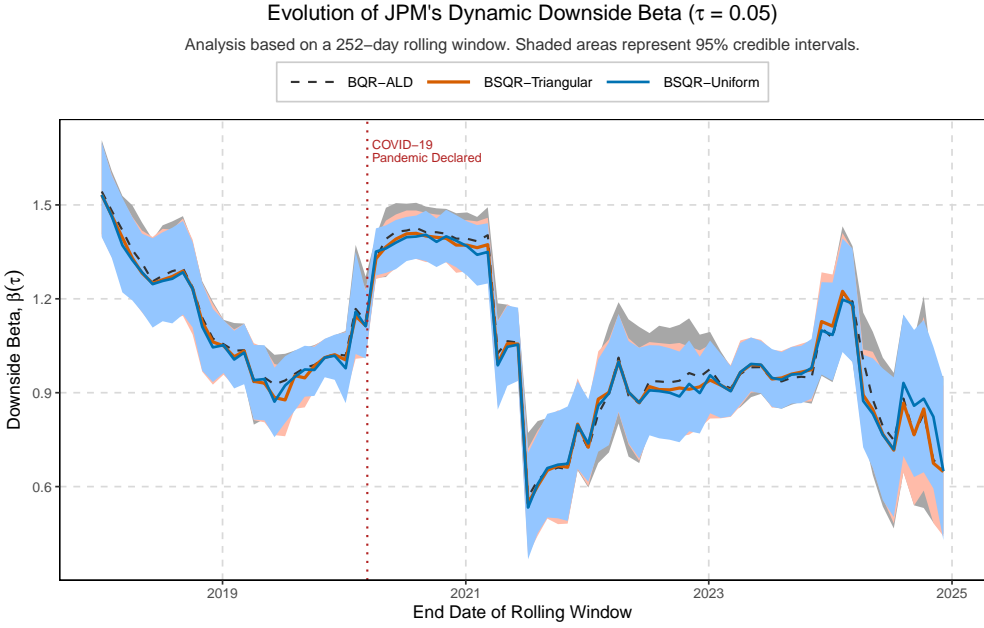
8.1 Inferential stability and economic insights from asymmetric betas

Methodologically, Figure 1 demonstrates that BSQR provides substantially more stable and interpretable parameter estimates. In both panels, the BQR-ALD benchmark produces visibly wider and more erratic credible intervals (light gray shaded area) plagued by high-frequency noise that can lead to over-interpretation of statistically insignificant fluctuations. In contrast, BSQR’s inherent kernel smoothing attenuates this noise, yielding tighter credible intervals (orange and blue shaded areas) and smoother posterior mean paths. This enables a more reliable quantification of uncertainty, clearly distinguishing genuine shifts in the risk profile from mere sampling variation.

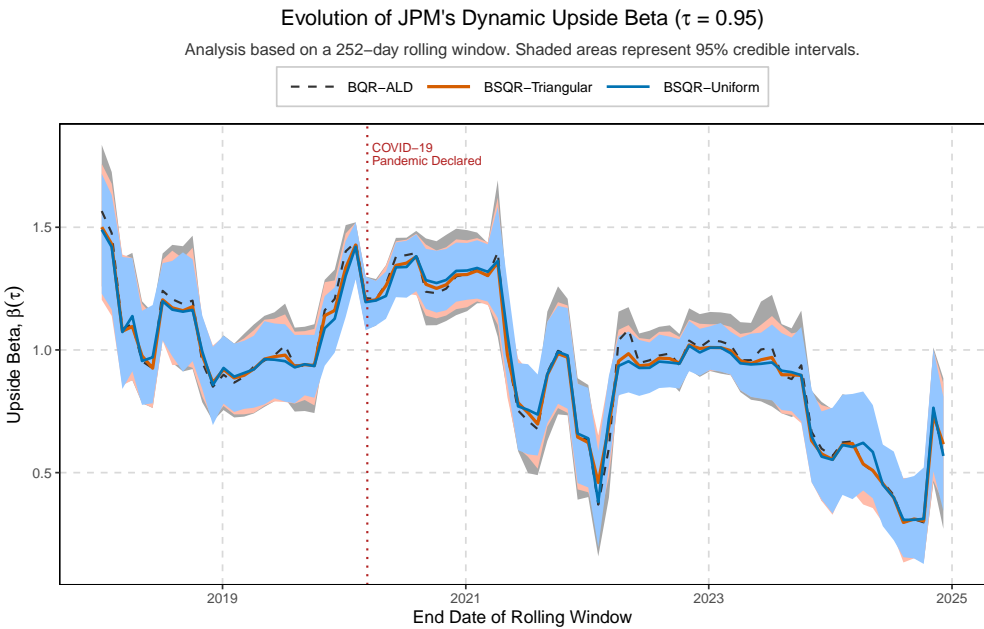
Economically, BSQR’s inferential clarity reveals a multi-phase and profoundly asymmetric response of JPM’s systemic risk to the COVID-19 shock. After an initial, transient symmetric spike in both betas during the early-2020 market panic, a more dominant and divergent dynamic quickly emerged. The downside beta ($\beta(0.05)$), previously stable around a pre-crisis baseline of roughly 0.97, decoupled from market downturns, plummeting to a trough of 0.53 by mid-2021 in a sustained “flight-to-quality” effect before settling into a new, lower regime averaging 0.92. In stark contrast, the upside beta ($\beta(0.95)$), originating from a similar 0.96 baseline, surged to a peak of 1.38 during the stimulus-fueled recovery, followed by a structural re-pricing that established a new, markedly lower equilibrium averaging 0.75. The superior stability of BSQR is what makes this nuanced dynamic sequence — a transient symmetric spike followed by a powerful asymmetric divergence — unambiguously clear.

8.2 Predictive accuracy and sampler efficiency

Beyond inferential quality, we assess BSQR’s out-of-sample predictive accuracy and computational efficiency. In terms of predictive accuracy, measured by the average one-day-ahead check loss, Table 2 shows that BSQR is highly competitive. For the downside quantile level ($\tau = 0.05$), the



(a) Evolution of the dynamic downside beta ($\beta(0.05)$) for JPM.



(b) Evolution of the dynamic upside beta ($\beta(0.95)$) for JPM.

Figure 1. Evolution of dynamic downside and upside systemic risk betas for JPM.

Note: Comparison of the benchmark (BQR-ALD) with BSQR methods (uniform and triangular kernels). The figures plot the posterior mean and 95% credible intervals for the (a) downside beta ($\tau = 0.05$) and (b) upside beta ($\tau = 0.95$), estimated using a 252-day rolling window. The BQR-ALD (benchmark) estimates exhibit wider and more volatile credible intervals compared to the smoother and tighter intervals from the BSQR methods.

Table 2. Out-of-sample forecasting performance for downside and upside quantile levels.

Methods	Downside ($\tau = 0.05$)	Upside ($\tau = 0.95$)
BQR-ALD	0.003027	0.001363
BSQR-Triangular	0.003031	0.001349
BSQR-Uniform	0.002998	0.001338

Table 3. MCMC sampler efficiency in rolling-window analysis.

Methods	Avg. Min. ESS	Avg. Time (s)	Avg. Divergences	Avg. Selected h
BQR-ALD	1399.66	0.77	0.00	NA
BSQR-Uniform	2554.72	0.69	0.00	0.60
BSQR-Triangular	2506.05	4.23	0.01	0.66

check loss of BSQR-Uniform (0.002998) and BSQR-Triangular (0.003031) is economically indistinguishable from that of BQR-ALD (0.003027). Notably, for the upside quantile level ($\tau = 0.95$), both BSQR methods (0.001338 and 0.001349) outperform the BQR-ALD benchmark (0.001363). This is a powerful result: BSQR’s substantial gains in inferential stability are achieved without sacrificing—and in the upside case, even enhancing—predictive accuracy.

Computationally, BSQR demonstrates superior sampler efficiency (Table 3). The average minimum effective sample size (Avg. Min. ESS), where higher values indicate more reliable posterior draws, for BSQR-Uniform (2554.72) and BSQR-Triangular (2506.05) is approximately 83% and 79% higher, respectively, than for BQR-ALD (1399.66), confirming that BSQR’s HMC-based sampler explores the posterior more effectively than BQR-ALD’s Gibbs sampler. While the BSQR-Triangular method’s enhanced quality comes at a higher computational cost (4.23s vs. 0.77s), BSQR remains the superior choice for applications where inferential robustness is paramount.

8.3 Robustness to bandwidth selection

To examine the influence of smoothing bandwidth (Section 7), we conducted a sensitivity analysis of the downside beta ($\beta(0.05)$) for a representative 252-day rolling window ending July 7, 2020, during significant market turmoil. Using the BSQR-Uniform method, we compared three bandwidths: the cross-validated choice ($h_{CV} \approx 1.08$), a smaller value ($h \approx 0.54$), and a larger one

($h \approx 2.16$). As shown in Figure 2, the posterior location of the systemic risk parameter is sensitive to h , with the mean shifting from about 1.36 to 1.42 as h increases, underscoring the need for a principled, data-driven bandwidth choice. Yet, despite this point-estimate sensitivity, the economic conclusion holds: all posterior distributions concentrate on values well above 1, confirming high systemic risk in the crisis period regardless of bandwidth. This analysis both quantifies model sensitivity and highlights the value of cross-validation as an objective, replicable criterion for balancing fit and smoothing.

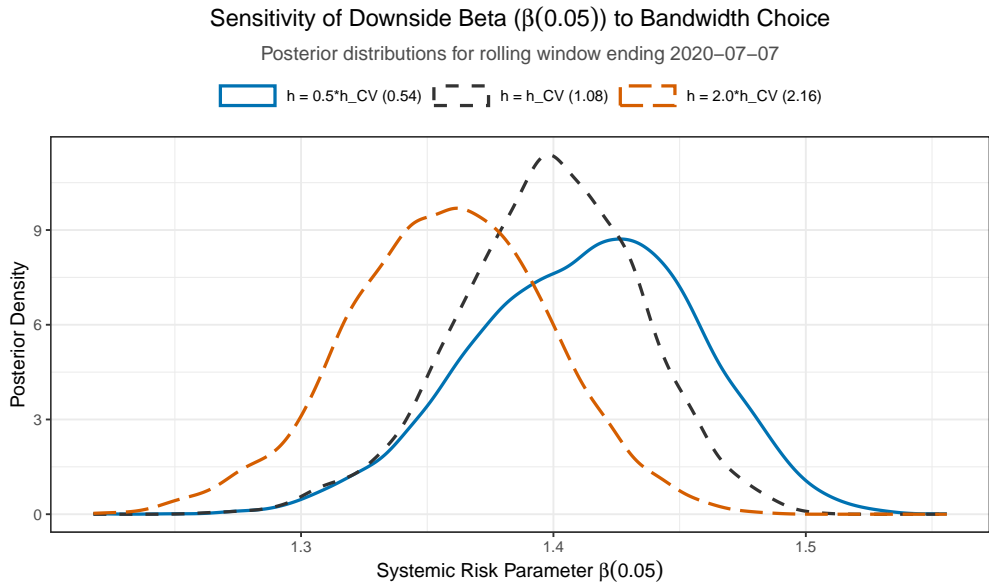


Figure 2. Sensitivity analysis of the downside beta ($\beta(0.05)$) to bandwidth choice. Posterior distributions for JPM are estimated on the 252-day window ending July 7, 2020, using three bandwidths (h). The bandwidth systematically shifts the posterior location, underscoring the value of data-driven selection such as cross-validation.

In aggregate, our empirical application shows BSQR to be a substantial methodological advance: it delivers more reliable and stable parameter estimates while maintaining competitive predictive performance. This enhanced inferential fidelity supports a more credible, nuanced understanding of economic phenomena, offering a powerful tool for researchers and practitioners prioritizing robustness.

9 Discussion

This paper introduces Bayesian smoothed quantile regression (BSQR), a framework resolving key inferential and computational challenges in Bayesian quantile modeling. By constructing a likelihood from a kernel-smoothed check loss, BSQR is both computationally efficient and inferentially sound: the proof of posterior consistency ensures correction of the inferential bias of standard BQR, while the smoothed likelihood enables modern HMC and NUTS sampling, a paradigm shift for scalable BQR. Analysis of posterior propriety under various priors clarifies the validity of Bayesian inference with smoothed loss, and links between compact-support kernels and tail equivalence with standard BQR posteriors offer further insight.

Future work includes multivariate extensions (Hallin et al., 2010), dynamic models with time-varying parameters (Gerlach et al., 2011), and deeper theory for bandwidth selection (Silverman, 1986). Even so, BSQR already represents a substantial advance: by smoothing the objective rather than approximating the posterior, it preserves Bayesian coherence while unlocking powerful computation. The combined strengths of proven consistency, empirical evidence, and sampler efficiency position BSQR as a valuable addition to the statistical toolkit. Its underlying principles—thoughtful smoothing, guaranteed asymptotic correctness, and computational efficiency—remain essential guideposts for researchers and practitioners.

Declaration of competing interest

The authors declare that they have no conflict of interest.

Author contributions

Bingqi Liu conceived the study, developed the BSQR framework, derived its theoretical properties, wrote the software, and conducted all numerical experiments. He also wrote the initial draft of the manuscript. Kangqiang Li provided assistance with the proofs of asymptotic posterior

consistency and kernel effects on posterior concentration. Tianxiao Pang supervised the research and provided critical feedback on the manuscript. All authors reviewed and approved the final manuscript.

Data and code availability

The source code and data required to replicate all numerical results in this paper are publicly available on GitHub at the following repository: <https://github.com/BeauquinLau/BSQR>.

References

Alhamzawi, R., & Ali, H. T. M. (2018). The Bayesian adaptive lasso regression. *Mathematical Biosciences*, 303, 75–82. doi: 10.1016/j.mbs.2018.06.004

Betancourt, M. (2017). A conceptual introduction to Hamiltonian Monte Carlo. *arXiv preprint arXiv:1701.02434*. doi: 10.48550/arXiv.1701.02434

Chernozhukov, V., Fernández-Val, I., & Melly, B. (2013). Inference on counterfactual distributions. *Econometrica*, 81(6), 2205–2268. doi: 10.3982/ECTA10582

Chernozhukov, V., & Hong, H. (2003). An MCMC approach to classical estimation. *Journal of Econometrics*, 115(2), 293–346. doi: 10.1016/S0304-4076(03)00100-3

Duane, S., Kennedy, A. D., Pendleton, B. J., & Roweth, D. (1987). Hybrid Monte Carlo. *Physics Letters B*, 195(2), 216–222. doi: 10.1016/0370-2693(87)91197-X

Fan, J., & Li, R. (2001). Variable selection via nonconcave penalized likelihood and its oracle properties. *Journal of the American Statistical Association*, 96(456), 1348–1360. doi: 10.1198/016214501753382273

Fernandes, M., Guerre, E., & Horta, E. (2021). Smoothing quantile regressions. *Journal of Business & Economic Statistics*, 39(1), 338–357. doi: 10.1080/07350015.2019.1660177

Gerlach, R. H., Chen, C. W. S., & Chan, N. Y. C. (2011). Bayesian time-varying quantile forecasting for Value-at-Risk in financial markets. *Journal of Business & Economic Statistics*, 29(4), 481–492. doi: 10.1198/jbes.2010.08203

Ghosal, S., Ghosh, J. K., & van der Vaart, A. W. (2000). Convergence rates of posterior distributions. *The Annals of Statistics*, 28(2), 500–531. doi: 10.1214/aos/1016218228

Gneiting, T. (2011). Making and evaluating point forecasts. *Journal of the American Statistical Association*, 106(494), 746–762. doi: 10.1198/jasa.2011.r10138

Hallin, M., Paindaveine, D., & Šiman, M. (2010). Multivariate quantiles and multiple-output regression quantiles: From L_1 optimization to halfspace depth. *The Annals of Statistics*, 38(2), 635–669. doi: 10.1214/09-AOS723

Hastings, W. K. (1970). Monte Carlo sampling methods using Markov chains and their applications. *Biometrika*, 57(1), 97–109. doi: 10.2307/2334940

Hoffman, M. D., & Gelman, A. (2014). The No-U-Turn sampler: Adaptively setting path lengths in Hamiltonian Monte Carlo. *Journal of Machine Learning Research*, 15, 1593–1623. Retrieved from <http://jmlr.org/papers/v15/hoffman14a.html>

Horowitz, J. L. (1998). *Semiparametric Methods in Econometrics* (Vol. 131). NY: Springer New York. doi: 10.1007/978-1-4612-0621-7

Koenker, R. (2005). *Quantile Regression*. Cambridge, UK: Cambridge University Press. doi: 10.1017/CBO9780511754098

Koenker, R., & Bassett, G. (1978). Regression quantiles. *Econometrica*, 46(1), 33–50. doi: 10.2307/1913643

Kozumi, H., & Kobayashi, G. (2011). Gibbs sampling methods for Bayesian quantile regression. *Journal of Statistical Computation and Simulation*, 81(11), 1565–1578. doi: 10.1080/00949655.2010.496117

Li, Q., Xi, R., & Lin, N. (2010). Bayesian regularized quantile regression. *Bayesian Analysis*, 5(3), 533–556. doi: 10.1214/10-BA521

Metropolis, N., Rosenbluth, A. W., Rosenbluth, M. N., Teller, A. H., & Teller, E. (1953). Equation of state calculations by fast computing machines. *The Journal of Chemical Physics*, 21(6), 1087–1092. doi: 10.1063/1.1699114

Neal, R. M. (2011). *MCMC Using Hamiltonian Dynamics*. NY: CRC Press. doi: 10.1201/b10905-6

Newey, W. K., & McFadden, D. (1994). Large sample estimation and hypothesis testing. In R. F. Engle & D. L. McFadden (Eds.), *Handbook of Econometrics, volume iv* (pp. 2111–2245). Elsevier. doi: 10.1016/S1573-4412(05)80005-4

Reich, B. J., Fuentes, M., & Dunson, D. B. (2011). Bayesian spatial quantile regression. *Journal of the American Statistical Association*, 106(493), 6–20. doi: 10.1198/jasa.2010.ap09237

Silverman, B. W. (1986). *Density Estimation for Statistics and Data Analysis*. London: Chapman and Hall. doi: 10.1007/978-1-4899-3324-9

Sriram, K., Ramamoorthi, R. V., & Ghosh, P. (2013). Posterior consistency of Bayesian quantile regression based on the misspecified asymmetric Laplace density. *Bayesian Analysis*, 8(2), 479–504. doi: 10.1214/13-BA817

Yang, Y., Wang, H. J., & He, X. (2016). Posterior inference in Bayesian quantile regression with asymmetric Laplace likelihood. *International Statistical Review*, 84(3), 327–344. doi: 10.1111/insr.12114

Yu, K., & Moyeed, R. A. (2001). Bayesian quantile regression. *Statistics & Probability Letters*, 54(4), 437–447. doi: 10.1016/S0167-7152(01)00124-9

Appendix A: Proofs

Proof of Theorem 1. The proof follows a standard strategy for demonstrating Bayesian posterior consistency (e.g., Chernozhukov & Hong, 2003; Ghosal et al., 2000). The approach consists of two key stages: first, we establish the consistency of the frequentist M-estimator, $\hat{\beta}_h(\tau)$, which minimizes the smoothed objective function $\hat{R}_h(\mathbf{b}; \tau, h)$. Second, we leverage this result to show that the full Bayesian posterior concentrates around the true parameter value.

The M-estimator $\hat{\beta}_h(\tau)$ is the minimizer of the sample objective function Eq. (7). To prove its consistency, we analyze its population analogue, $R_h(\mathbf{b}; \tau, h) := \mathbb{E}[\hat{R}_h(\mathbf{b}; \tau, h)]$, and show that it is uniquely minimized at the true parameter $\beta_0(\tau)$ as $n \rightarrow \infty$. First, we analyze the gradient of the population objective function with respect to \mathbf{b} , which is $\nabla_{\mathbf{b}} R_h(\mathbf{b}; \tau, h) = \mathbb{E}[-\mathbf{x}_i \Psi_h(\mathbf{e}_i(\mathbf{b}); \tau)]$ by using the definition Eq. (8). Evaluating this at the true parameter $\mathbf{b} = \beta_0(\tau)$ yields:

$$\nabla_{\beta_0(\tau)} R_h(\beta_0(\tau); \tau, h) = \mathbb{E}[-\mathbf{x}_i \Psi_h(\varepsilon_{0i}; \tau)] = -\mathbb{E}_{\mathbf{x}}[\mathbf{x}_i] \cdot \mathbb{E}_{\varepsilon}[\Psi_h(\varepsilon_{0i}; \tau)],$$

where the final equality uses the independence of \mathbf{x}_i and ε_{0i} . The central task is to evaluate the expectation of the score function, $\mathbb{E}_{\varepsilon}[\Psi_h(\varepsilon_{0i}; \tau)]$, which is calculated as follows:

$$\begin{aligned} \mathbb{E}_{\varepsilon}[\Psi_h(\varepsilon_{0i}; \tau)] &= \mathbb{E} \left[\int_{-\infty}^{\infty} \psi_{\tau}(\varepsilon_{0i} - v) K_h(v) dv \right] = \int_{-\infty}^{\infty} \mathbb{E}[\tau - \mathbb{I}(\varepsilon_{0i} < v)] K_h(v) dv \\ &= \int_{-\infty}^{\infty} (\tau - F_{\varepsilon}(v)) K_h(v) dv = \int_{-\infty}^{\infty} (\tau - F_{\varepsilon}(zh)) K(z) dz. \end{aligned}$$

By **Assumption (C2a)**, $F_{\varepsilon}(u)$ is twice differentiable around 0, allowing a second-order Taylor expansion: $F_{\varepsilon}(u) = F_{\varepsilon}(0) + u f_{\varepsilon}(0) + \frac{u^2}{2} f'_{\varepsilon}(0) + o(u^2)$. Since the model definition implies $F_{\varepsilon}(0) = \tau$, we substitute $u = zh$ into the integral and obtain that

$$\begin{aligned} \mathbb{E}_{\varepsilon}[\Psi_h(\varepsilon_{0i}; \tau)] &= \int_{-\infty}^{\infty} \left(\tau - \left[\tau + (zh) f_{\varepsilon}(0) + \frac{(zh)^2}{2} f'_{\varepsilon}(0) + o((zh)^2) \right] \right) K(z) dz \\ &= -h f_{\varepsilon}(0) \int_{-\infty}^{\infty} z K(z) dz - \frac{h^2}{2} f'_{\varepsilon}(0) \int_{-\infty}^{\infty} z^2 K(z) dz + o(h^2) \end{aligned}$$

$$= 0 - O(h^2) = O(h^2)$$

by utilizing $\int_{-\infty}^{\infty} z K(z) dz = 0$ in **Assumption (C4)**. Thus, $\nabla_{\beta_0(\tau)} R_h(\beta_0(\tau); \tau, h) = O(h^2)$, which converges to $\mathbf{0}$ as $n \rightarrow \infty$ due to $h \rightarrow 0$.

Next, we verify the second-order condition by examining the Hessian matrix of $R_h(\mathbf{b}; \tau, h)$ at $\beta_0(\tau)$, denoted as $\mathbf{H}_h(\beta_0(\tau))$. Note that

$$\mathbf{H}_h(\mathbf{b}) := \nabla_{\mathbf{b}}^2 R_h(\mathbf{b}; \tau, h) = \mathbb{E}[\mathbf{x}_i \mathbf{x}_i^\top \cdot \Psi'_h(e_i(\mathbf{b}); \tau)].$$

At $\mathbf{b} = \beta_0(\tau)$, we have $\Psi'_h(\varepsilon_{0i}; \tau) = K_h(\varepsilon_{0i})$. As $n \rightarrow \infty$ and $h \rightarrow 0$, the expectation $\mathbb{E}[\Psi'_h(\varepsilon_{0i}; \tau)] = \int_{-\infty}^{\infty} K_h(u) f_\varepsilon(u) du$ converges to $f_\varepsilon(0)$. Consequently, the Hessian matrix:

$$\mathbf{H}_h(\beta_0(\tau)) \rightarrow \mathbb{E}[\mathbf{x}_i \mathbf{x}_i^\top f_\varepsilon(0)] = f_\varepsilon(0) \mathbb{E}[\mathbf{x}_i \mathbf{x}_i^\top] = f_\varepsilon(0) \Sigma_X.$$

This limiting matrix is positive definite, since $f_\varepsilon(0) > 0$ by **Assumption (C2a)** and Σ_X is positive definite by **Assumption (C3)**.

Since the population objective function $R_h(\mathbf{b}; \tau, h)$ has a gradient that converges to zero and a positive definite Hessian at $\beta_0(\tau)$, $\beta_0(\tau)$ is the unique minimizer of $R_h(\mathbf{b}; \tau, h)$ in the limit. To establish that $\hat{\beta}_h(\tau) \xrightarrow{P} \beta_0(\tau)$, M-estimation theory requires showing that $\sup_{\mathbf{b} \in \mathcal{B}} |\hat{R}_h(\mathbf{b}; \tau, h) - R_h(\mathbf{b}; \tau, h)| \xrightarrow{P} 0$. This uniform convergence is guaranteed by the uniform law of large numbers (ULLN), for which we must verify the existence of a dominating function for $L_h(e_i(\mathbf{b}); \tau)$ with a finite expectation. The argument of the loss function is $e_i(\mathbf{b}) = y_i - \mathbf{x}_i^\top \mathbf{b} = \varepsilon_{0i} - \mathbf{x}_i^\top (\mathbf{b} - \beta_0(\tau))$. Since the magnitude of L_h is bounded by a multiple of its argument, the task reduces to uniformly bounding $|e_i(\mathbf{b})|$ over the compact set \mathcal{B} :

$$\sup_{\mathbf{b} \in \mathcal{B}} |e_i(\mathbf{b})| \leq |\varepsilon_{0i}| + \sup_{\mathbf{b} \in \mathcal{B}} |\mathbf{x}_i^\top (\mathbf{b} - \beta_0(\tau))| \leq |\varepsilon_{0i}| + \|\mathbf{x}_i\| \sup_{\mathbf{b} \in \mathcal{B}} \|\mathbf{b} - \beta_0(\tau)\|.$$

The inequality above shows that this bound depends on two key terms, both of which are

controlled by our assumptions. First, the term $\sup_{\beta \in \mathcal{B}} \|\beta - \beta_0(\tau)\|$ is bounded by the diameter of the parameter space, $D_{\mathcal{B}}$, because \mathcal{B} is assumed to be compact (**Assumption (C1)**). Second, the covariate norm $\|\mathbf{x}_i\|$ is uniformly bounded by a constant M_X (**Assumption (C3)**). These assumptions jointly allow us to construct a dominating function $D_i = C \cdot (|\varepsilon_{0i}| + M_X D_{\mathcal{B}})$ for some constant $C > 0$. The final condition is to ensure its expectation, $\mathbb{E}[D_i]$, is finite. This is guaranteed by **Assumption (C2b)**, which explicitly requires that the error term ε_{0i} has a finite first moment. With all conditions for the ULLN satisfied, the uniform convergence of the objective function is established. The consistency of the M-estimator, $\hat{\beta}_h(\tau) \xrightarrow{P} \beta_0(\tau)$, then follows directly from standard large-sample theory (Newey & McFadden, 1994).

With these frequentist properties established, the proof of posterior consistency follows a standard argument. The Bayesian analysis employs a quasi-likelihood function constructed from the M-estimation objective: $L(\beta, \theta | \mathbf{y}, \mathbf{X}) \propto \exp(-n\theta \widehat{R}_h(\beta; \tau, h))$. The properties we have just demonstrated are precisely the conditions that ensure this quasi-likelihood concentrates its mass in a shrinking neighborhood of the true parameter. Combined with a prior distribution $\pi(\beta)$ that assigns positive mass to any such neighborhood (**Assumption (C5)**), established theorems in Bayesian asymptotics (e.g., Theorem 1 in Chernozhukov & Hong, 2003; see also Theorem 2.1 in Ghosal et al., 2000) confirm that the posterior distribution inherits this concentration property. Consequently, the posterior distribution $\pi(\beta | \mathbf{y}, \mathbf{X}, \theta)$ contracts to a point mass at the true parameter $\beta_0(\tau)$. \square

Proof of Theorem 2. Proof of Part (i). Let $I_1 = \int_{\mathbb{R}^d} L(\mathbf{y} | \mathbf{X}, \beta, \theta; \tau, h) \pi(\beta) d\beta$. From Eq. (11), we can express I_1 as:

$$I_1 \propto (Z(\theta, \tau, h))^{-n} \int_{\mathbb{R}^d} \exp(-\theta S(\beta; \tau, h)) d\beta.$$

Since $L_h(e; \tau) = (\rho_\tau * K_h)(e) \geq 0$ (due to the non-negativity of ρ_τ and K_h), it follows that $S(\beta; \tau, h) \geq 0$. The integrand $\exp(-\theta S(\beta; \tau, h))$ is continuous and strictly positive, and $(Z(\theta, \tau, h))^{-n} > 0$, which implies $I_1 > 0$.

To establish the finiteness of I_1 , we begin by deriving a lower bound for $L_h(e; \tau)$. The check

function $\rho_\tau(u)$ satisfies $\rho_\tau(u) \geq \min(\tau, 1 - \tau)|u|$. Letting $c_\tau = \min(\tau, 1 - \tau) > 0$, we obtain the following lower bound for the smoothed loss:

$$\begin{aligned} L_h(e; \tau) &= \int_{-\infty}^{\infty} \rho_\tau(e - v) K_h(v) dv \geq c_\tau \int_{-\infty}^{\infty} |e - v| K_h(v) dv \geq c_\tau \int_{-\infty}^{\infty} (|e| - |v|) K_h(v) dv \\ &= c_\tau |e| \int_{-\infty}^{\infty} K_h(v) dv - c_\tau \int_{-\infty}^{\infty} |v| K_h(v) dv = c_\tau |e| - c_\tau \int_{-\infty}^{\infty} |v| \frac{1}{h} K\left(\frac{v}{h}\right) dv \\ &= c_\tau (|e| - h M_K) \end{aligned}$$

by applying the reverse triangle inequality $|e - v| \geq |e| - |v|$ and the substitution $u = v/h$, where $M_K = \int_{-\infty}^{\infty} |u| K(u) du$ is finite by assumption. More precisely, there exist constants $c_1 = c_\tau > 0$ and $C_1 = c_\tau h M_K \geq 0$ such that $L_h(e; \tau) \geq c_1 |e| - C_1$ for all e .

Next, we derive a lower bound for $S(\beta; \tau, h)$. Summing over all observations gives

$$S(\beta; \tau, h) \geq \sum_{i=1}^n (c_1 |y_i - \mathbf{x}_i^\top \beta| - C_1) = c_1 \|\mathbf{y} - \mathbf{X}\beta\|_1 - nC_1.$$

By norm equivalence, there exists $c_2 > 0$ such that $\|z\|_1 \geq c_2 \|z\|_2$, which implies $S(\beta; \tau, h) \geq c_1 c_2 \|\mathbf{y} - \mathbf{X}\beta\|_2 - nC_1$. Using the reverse triangle inequality, we have $\|\mathbf{y} - \mathbf{X}\beta\|_2 \geq \|\mathbf{X}\beta\|_2 - \|\mathbf{y}\|_2$. Since the design matrix \mathbf{X} has full column rank d , the mapping $\beta \mapsto \mathbf{X}\beta$ is injective. This implies that $\|\mathbf{X}\beta\|_2$ defines a norm on \mathbb{R}^d . By norm equivalence on \mathbb{R}^d , there exists $c_3 > 0$ such that $\|\mathbf{X}\beta\|_2 \geq c_3 \|\beta\|_2$. Combining these, we obtain for sufficiently large $\|\beta\|_2$:

$$S(\beta; \tau, h) \geq c_1 c_2 (c_3 \|\beta\|_2 - \|\mathbf{y}\|_2) - nC_1 = (c_1 c_2 c_3) \|\beta\|_2 - (c_1 c_2 \|\mathbf{y}\|_2 + nC_1).$$

Letting $c_4 = c_1 c_2 c_3 > 0$ and $C_2 = c_1 c_2 \|\mathbf{y}\|_2 + nC_1 \geq 0$, we have the linear growth condition:

$$S(\beta; \tau, h) \geq c_4 \|\beta\|_2 - C_2.$$

This growth rate ensures the exponential decay of the integrand:

$$\exp(-\theta S(\beta; \tau, h)) \leq \exp(-\theta(c_4 \|\beta\|_2 - C_2)) = Ce^{-A\|\beta\|_2},$$

where $A = \theta c_4 > 0$ and $C = e^{\theta C_2} > 0$.

To evaluate the integral $\int_{\mathbb{R}^d} e^{-A\|\beta\|_2} d\beta$, we employ d -dimensional hyperspherical coordinates. Letting $r = \|\beta\|_2$, the volume element becomes $d\beta = r^{d-1} dr d\Omega_{d-1}$, where $d\Omega_{d-1}$ is the surface element on the unit $(d-1)$ -sphere. Thus,

$$\begin{aligned} \int_{\mathbb{R}^d} e^{-A\|\beta\|_2} d\beta &= \int_{\Omega_{d-1}} \int_0^\infty e^{-Ar} r^{d-1} dr d\Omega_{d-1} = \left(\int_{\Omega_{d-1}} d\Omega_{d-1} \right) \left(\int_0^\infty e^{-Ar} r^{d-1} dr \right) \\ &= S_{d-1} \int_0^\infty e^{-Ar} r^{d-1} dr, \end{aligned}$$

where $S_{d-1} = 2\pi^{d/2}/\Gamma(d/2)$ is the surface area of the unit $(d-1)$ -sphere. The substitution $t = Ar$ yields

$$\int_0^\infty e^{-Ar} r^{d-1} dr = \int_0^\infty e^{-t} \left(\frac{t}{A} \right)^{d-1} \frac{1}{A} dt = \frac{1}{A^d} \int_0^\infty t^{d-1} e^{-t} dt = \frac{\Gamma(d)}{A^d} = \frac{(d-1)!}{A^d},$$

since d is a positive integer. Therefore, the integral of the non-negative function $\exp(-\theta S(\beta; \tau, h))$ is

$$\int_{\mathbb{R}^d} \exp(-\theta S(\beta; \tau, h)) d\beta \leq \int_{\mathbb{R}^d} Ce^{-A\|\beta\|_2} d\beta = C \int_{\mathbb{R}^d} e^{-A\|\beta\|_2} d\beta = CS_{d-1} \frac{(d-1)!}{A^d} < \infty.$$

Since $\exp(-\theta S(\beta; \tau, h))$ is non-negative and dominated by the integrable function $Ce^{-A\|\beta\|_2}$, the comparison test guarantees the convergence of I_1 . Combined with the earlier result $I_1 > 0$, we conclude that $0 < I_1 < \infty$, establishing the propriety of the posterior distribution $\pi(\beta | \mathbf{y}, \mathbf{X}, \theta)$.

Proof of Part (ii). The joint posterior distribution satisfies

$$\pi(\beta, \theta | \mathbf{y}, \mathbf{X}) \propto (Z(\theta, \tau, h))^{-n} \exp(-\theta S(\beta; \tau, h)) \pi(\theta),$$

with propriety requiring the normalization integral

$$J_1 := \int_0^\infty (Z(\theta, \tau, h))^{-n} I_\beta(\theta) \pi(\theta) d\theta \quad (\text{A.1})$$

to be finite and positive, where $I_\beta(\theta) := \int_{\mathbb{R}^d} \exp(-\theta S(\beta; \tau, h)) d\beta$. From the proof of Theorem 2(i), we know that there exist constants $c_L > 0$ and $C_S \geq 0$ such that $S(\beta; \tau, h) \geq c_L \|\beta\|_2 - C_S$. This yields the bound

$$\exp(-\theta S(\beta; \tau, h)) \leq \exp(-\theta(c_L \|\beta\|_2 - C_S)) = e^{\theta C_S} \exp(-\theta c_L \|\beta\|_2).$$

Hence $I_\beta(\theta)$ is dominated by

$$I_\beta(\theta) \leq e^{\theta C_S} \int_{\mathbb{R}^d} \exp(-\theta c_L \|\beta\|_2) d\beta. \quad (\text{A.2})$$

The radial integral evaluates via hyperspherical coordinates to $\int_{\mathbb{R}^d} \exp(-\alpha \|x\|_2) dx = \frac{2\pi^{d/2}}{\Gamma(d/2)} \Gamma(d) \alpha^{-d}$ for $\alpha > 0$. Substituting $\alpha = \theta c_L$ we obtain the upper bound for Eq. (A.2):

$$I_\beta(\theta) \leq K_1 e^{\theta C_S} \theta^{-d}, \quad K_1 = \frac{2\pi^{d/2} \Gamma(d)}{\Gamma(d/2) c_L^d} > 0.$$

Thus, substitution into (A.1) yields the sufficient condition (13):

$$J_1 \leq K_1 \int_0^\infty \frac{\pi(\theta) e^{\theta C_S}}{(Z(\theta, \tau, h))^n \theta^d} d\theta < \infty.$$

Now, consider the specific case where the prior for θ is a Gamma distribution, $\pi(\theta) = \frac{b^a}{\Gamma(a)} \theta^{a-1} e^{-b\theta}$, for $a > 0, b > 0$. To establish the propriety of the joint posterior, it is sufficient to show that the integral of its upper bound, as derived from the bound on $I_\beta(\theta)$, is finite. Let's analyze the integrand of this bounding integral:

$$\frac{\pi(\theta) e^{\theta C_S}}{(Z(\theta, \tau, h))^n \theta^d} = \frac{b^a}{\Gamma(a)} \theta^{a-1} e^{-b\theta} \cdot \frac{e^{\theta C_S}}{(Z(\theta, \tau, h))^n \theta^d}$$

$$= \frac{b^a}{\Gamma(a)} (Z(\theta, \tau, h))^{-n} \theta^{a-d-1} e^{-(b-C_S)\theta}.$$

The convergence of the integral of this expression over $(0, \infty)$ depends on its asymptotic behavior as $\theta \rightarrow \infty$ and $\theta \rightarrow 0$:

1. **Behavior as $\theta \rightarrow \infty$:** To establish the convergence condition for large θ , we first examine the asymptotic behavior of $(Z(\theta, \tau, h))^{-n}$. This entails applying Laplace's method to $Z(\theta, \tau, h)$, which exploits the fact that, for large θ , the integrand $e^{-\theta L_h(u; \tau)}$ concentrates sharply around the global minimum of $L_h(u; \tau)$. By assumption in Theorem 2(ii), this minimum is $L_{\min} > 0$ and achieved at a unique point u_{\min} . The Taylor expansion of $L_h(u; \tau)$ around u_{\min} yields

$$L_h(u; \tau) = L_{\min} + \frac{L''_h(u_{\min}; \tau)}{2}(u - u_{\min})^2 + O((u - u_{\min})^3).$$

The leading asymptotic contribution to $Z(\theta, \tau, h)$ arises from integrating the exponential of the constant and quadratic terms:

$$\int_{-\infty}^{\infty} \exp\left(-\theta \left[L_{\min} + \frac{L''_h(u_{\min}; \tau)}{2}(u - u_{\min})^2\right]\right) du = e^{-\theta L_{\min}} \int_{-\infty}^{\infty} \exp\left(-\frac{\theta L''_h(u_{\min}; \tau)}{2}(u - u_{\min})^2\right) du.$$

The integral evaluates to the Gaussian form $\sqrt{2\pi/(\theta L''_h(u_{\min}; \tau))}$. Laplace's method formalizes that the full integral $Z(\theta, \tau, h)$ equals this leading term times a factor approaching 1, incorporating higher-order corrections:

$$Z(\theta, \tau, h) = \sqrt{\frac{2\pi}{L''_h(u_{\min}; \tau)}} \theta^{-1/2} e^{-\theta L_{\min}} (1 + o(1)).$$

Consequently,

$$\begin{aligned} (Z(\theta, \tau, h))^{-n} &= \left(\sqrt{\frac{2\pi}{L''_h(u_{\min}; \tau)}} \theta^{-1/2} e^{-\theta L_{\min}} (1 + o(1)) \right)^{-n} \\ &= C \cdot \theta^{n/2} e^{nL_{\min}\theta} (1 + o(1)), \end{aligned}$$

where the constant $C = (L''_h(u_{\min}; \tau)/(2\pi))^{n/2} > 0$ absorbs the prefactor, and $(1 + o(1))^{-n} = 1 + o(1)$ for fixed n . Disregarding the constant $\frac{b^a}{\Gamma(a)}$, the relevant expression becomes

$$\begin{aligned} (Z(\theta, \tau, h))^{-n} \theta^{a-d-1} e^{-(b-C_S)\theta} &= C \cdot \theta^{n/2} e^{nL_{\min}\theta} (1 + o(1)) \cdot \theta^{a-d-1} \cdot e^{-(b-C_S)\theta} \\ &= C \cdot \theta^{a+n/2-d-1} e^{-(b-C_S-nL_{\min})\theta} (1 + o(1)). \end{aligned}$$

For the integral over θ to converge as the upper limit tends to infinity, the integrand must decay. The exponential $e^{-(b-C_S-nL_{\min})\theta}$ dominates the polynomial terms for large θ , necessitating a positive coefficient for exponential decay:

$$b - C_S - nL_{\min} > 0 \implies b > C_S + nL_{\min}.$$

2. Behavior as $\theta \rightarrow 0$: Near zero, we use the assumption that $(Z(\theta, \tau, h))^{-n} = O(\theta^{k_Z})$ for some constant k_Z . The integrand's behavior is therefore dominated by the polynomial term:

$$O(\theta^{k_Z}) \cdot \theta^{a-d-1} e^{-(b-C_S)\theta} \sim O(\theta^{a+k_Z-d-1}).$$

For an integral of the form $\int_0^\epsilon \theta^p d\theta$ to converge, the exponent must satisfy $p > -1$. Applying this to our case, we require:

$$a + k_Z - d - 1 > -1 \implies a + k_Z > d.$$

Both conditions must hold simultaneously to guarantee the convergence of the bounding integral. Therefore, for a $\text{Gamma}(a, b)$ prior on θ , the joint posterior distribution $\pi(\beta, \theta | \mathbf{y}, \mathcal{X})$ is proper if $b > C_S + nL_{\min}$ and $a + k_Z > d$. \square

Proof of Theorem 3. Proof of Part (i). The integral of interest, ignoring proportionality constants

from the likelihood not involving β , is

$$I_2 := \int_{\mathbb{R}^d} \exp(-\theta S(\beta; \tau, h)) \exp\left(-\frac{\|\beta\|_2^2}{2\sigma_\beta^2}\right) d\beta.$$

Let $g(\beta) = \exp\left(-\theta S(\beta; \tau, h) - \|\beta\|_2^2/(2\sigma_\beta^2)\right)$. Since $S(\beta; \tau, h) \geq 0$ and $\theta > 0$, the term $\exp(-\theta S(\beta; \tau, h))$ is strictly positive and bounded above by 1. The Gaussian prior term $\exp(-\|\beta\|_2^2/(2\sigma_\beta^2))$ is strictly positive. Thus, $g(\beta)$ is strictly positive and continuous. Its integral over \mathbb{R}^d must therefore be strictly positive, ensuring $I_2 > 0$.

To establish finiteness, we use the comparison test. Since $-\theta S(\beta; \tau, h) \leq 0$, we have

$$-\theta S(\beta; \tau, h) - \frac{\|\beta\|_2^2}{2\sigma_\beta^2} \leq -\frac{\|\beta\|_2^2}{2\sigma_\beta^2}.$$

Exponentiating gives $g(\beta) \leq \exp\left(-\frac{\|\beta\|_2^2}{2\sigma_\beta^2}\right)$. The integral of this upper bound is $\int_{\mathbb{R}^d} \exp\left(-\frac{\|\beta\|_2^2}{2\sigma_\beta^2}\right) d\beta = (2\pi\sigma_\beta^2)^{d/2}$, which is finite. By comparison, I_2 is also finite. Thus, $0 < I_2 < \infty$, and the posterior is proper.

Proof of Part (ii). The joint posterior is proportional to

$$\pi(\beta, \theta | \mathbf{y}, \mathbf{X}, \sigma_\beta^2, a_\theta, b_\theta) \propto (Z(\theta, \tau, h))^{-n} \exp(-\theta S(\beta; \tau, h)) \pi(\beta | \sigma_\beta^2) \pi(\theta | a_\theta, b_\theta).$$

The joint posterior density is proportional to

$$\pi(\beta, \theta | \mathbf{y}, \mathbf{X}, \sigma_\beta^2) \propto L(\mathbf{y} | \mathbf{X}, \beta, \theta) \pi(\beta | \sigma_\beta^2) \pi(\theta).$$

Substituting the likelihood form $L(\mathbf{y} | \mathbf{X}, \beta, \theta; \tau, h)$ as showed in Eq. (11), we have

$$\pi(\beta, \theta | \mathbf{y}, \mathbf{X}, \sigma_\beta^2) \propto (Z(\theta, \tau, h))^{-n} \exp(-\theta S(\beta; \tau, h)) \pi(\beta | \sigma_\beta^2) \pi(\theta).$$

To show propriety, we need to demonstrate that the integral of this joint posterior over β and θ is

finite and positive:

$$J_2 := \int_0^\infty \int_{\mathbb{R}^d} (Z(\theta, \tau, h))^{-n} \exp(-\theta S(\beta; \tau, h)) \pi(\beta \mid \sigma_\beta^2) \pi(\theta) d\beta d\theta.$$

Since the integrand is non-negative, we can apply Tonelli's theorem to change the order of integration:

$$J_2 = \int_0^\infty (Z(\theta, \tau, h))^{-n} \pi(\theta) \left(\int_{\mathbb{R}^d} \exp(-\theta S(\beta; \tau, h)) \pi(\beta \mid \sigma_\beta^2) d\beta \right) d\theta.$$

Note that $\pi(\beta \mid \sigma_\beta^2) = (2\pi\sigma_\beta^2)^{-d/2} \exp\left(-\frac{\|\beta\|_2^2}{2\sigma_\beta^2}\right)$, so the inner integral is $(2\pi\sigma_\beta^2)^{-d/2} I_2$, where I_2 has been defined in part (i). Thus,

$$J_2 = \int_0^\infty (Z(\theta, \tau, h))^{-n} \pi(\theta) \cdot (2\pi\sigma_\beta^2)^{-d/2} I_2 d\theta.$$

From the proof of part (i) of this theorem, we established that for any fixed $\theta > 0$, $0 < I_2(\theta) < \infty$. Specifically, it was shown that $I_2(\theta) \leq \int_{\mathbb{R}^d} \exp\left(-\frac{\|\beta\|_2^2}{2\sigma_\beta^2}\right) d\beta = (2\pi\sigma_\beta^2)^{d/2}$. Substituting this inequality into the expression for J_2 :

$$0 < J_2 \leq (2\pi\sigma_\beta^2)^{-d/2} \cdot (2\pi\sigma_\beta^2)^{d/2} \int_0^\infty (Z(\theta, \tau, h))^{-n} \pi(\theta) d\theta = \int_0^\infty (Z(\theta, \tau, h))^{-n} \pi(\theta) d\theta.$$

Therefore, if the integral $\int_0^\infty (Z(\theta, \tau, h))^{-n} \pi(\theta) d\theta$ converges to a finite positive value, then J_2 is also finite and positive, ensuring the joint posterior is proper. The strict positivity of J_2 is guaranteed because $(Z(\theta, \tau, h))^{-n} > 0$, $\pi(\theta) \geq 0$ (and integrates to 1, so not identically zero), and $I_2 > 0$.

For the specific instance where $\pi(\theta \mid a_\theta, b_\theta)$ is a Gamma distribution with $a_\theta > 0$ and $b_\theta > 0$.

The condition for propriety becomes the convergence of

$$\int_0^\infty (Z(\theta, \tau, h))^{-n} \frac{b_\theta^{a_\theta}}{\Gamma(a_\theta)} \theta^{a_\theta-1} e^{-b_\theta\theta} d\theta.$$

Since $b_\theta^{a_\theta}/\Gamma(a_\theta)$ is a positive constant, this is equivalent to the convergence of

$$\int_0^\infty (Z(\theta, \tau, h))^{-n} \theta^{a_\theta-1} e^{-b_\theta \theta} d\theta$$

to a finite positive value. \square

Proof of Proposition 1. Proof of Part (i). The derivative of $Z(\theta, \tau, h)$ with respect to θ is found by differentiating under the integral sign. This interchange of operations is justified by the Leibniz integral rule provided the partial derivative of the integrand is bounded in magnitude by an integrable function. For any θ in a compact interval $[a, b]$ with $0 < a < b < \infty$, we can establish such a bound:

$$\left| \frac{\partial}{\partial \theta} \exp(-\theta L_h(u; \tau)) \right| = L_h(u; \tau) \exp(-\theta L_h(u; \tau)) \leq L_h(u; \tau) \exp(-a L_h(u; \tau)).$$

The dominating function on the right-hand side is integrable on \mathbb{R} because, due to the exponential factor, it approaches zero as $|u| \rightarrow \infty$ at a rate faster than any inverse polynomial (e.g., faster than $1/u^2$). The conditions for the Leibniz rule are therefore met, and we can write:

$$\frac{\partial Z(\theta, \tau, h)}{\partial \theta} = \int_{-\infty}^\infty -L_h(u; \tau) \exp(-\theta L_h(u; \tau)) du.$$

Since $\exp(-\theta L_h(u; \tau)) > 0$ and $L_h(u; \tau)$ is non-negative and not identically zero, the integrand is non-positive and strictly negative on a set of non-zero measure. Therefore, $\partial Z(\theta, \tau, h)/\partial \theta < 0$, establishing strict decrease.

Proof of Part (ii). To show convexity of $\log Z(\theta, \tau, h)$, we examine its second derivative with respect to θ . The first-order partial derivative of $\log Z(\theta, \tau, h)$ with respect to θ is:

$$\frac{\partial \log Z(\theta, \tau, h)}{\partial \theta} = \frac{1}{Z(\theta, \tau, h)} \frac{\partial Z(\theta, \tau, h)}{\partial \theta} = \frac{\int_{-\infty}^\infty -L_h(u; \tau) e^{-\theta L_h(u; \tau)} du}{\int_{-\infty}^\infty e^{-\theta L_h(u; \tau)} du} = -\mathbb{E}_{p_u}[L_h(u; \tau)],$$

where $p_u(u \mid \theta) = \frac{\exp(-\theta L_h(u; \tau))}{Z(\theta, \tau, h)}$ can be interpreted as a probability density for u parameterized by θ .

The same justification allows for a second differentiation under the integral sign, and we have

$$\begin{aligned}
& \frac{\partial^2 \log Z(\theta, \tau, h)}{\partial \theta^2} \\
&= \frac{\partial}{\partial \theta} \left(\frac{\int_{-\infty}^{\infty} -L_h(u; \tau) e^{-\theta L_h(u; \tau)} du}{Z(\theta, \tau, h)} \right) \\
&= \frac{\left(\int_{-\infty}^{\infty} L_h^2(u; \tau) e^{-\theta L_h(u; \tau)} du \right) Z(\theta, \tau, h) - \left(\int_{-\infty}^{\infty} -L_h(u; \tau) e^{-\theta L_h(u; \tau)} du \right) \left(\int_{-\infty}^{\infty} -L_h(u; \tau) e^{-\theta L_h(u; \tau)} du \right)}{Z(\theta, \tau, h)^2} \\
&= \int_{-\infty}^{\infty} L_h(u; \tau)^2 \frac{e^{-\theta L_h(u; \tau)}}{Z(\theta, \tau, h)} du - \left(\int_{-\infty}^{\infty} -L_h(u; \tau) \frac{e^{-\theta L_h(u; \tau)}}{Z(\theta, \tau, h)} du \right)^2 \\
&= \mathbb{E}_{p_u} [L_h(u; \tau)^2] - (\mathbb{E}_{p_u} [L_h(u; \tau)])^2 = \text{Var}_{p_u} (L_h(u; \tau)).
\end{aligned}$$

Since variance is always non-negative, we have $\frac{\partial^2 \log Z(\theta, \tau, h)}{\partial \theta^2} \geq 0$. This confirms the convexity of $\log Z(\theta, \tau, h)$ with respect to θ . \square

Proof of Theorem 4. The posterior distributions are given by:

$$\begin{aligned}
\pi_{\text{BSQR}}(\boldsymbol{\beta} \mid \theta, \mathbf{y}, \mathbf{X}; \tau, h) &= \frac{1}{Z_{\text{BSQR}}(\theta, h, \pi)} \exp \left(-\theta \sum_{i=1}^n L_h(e_i(\boldsymbol{\beta}); \tau) \right) \pi(\boldsymbol{\beta}), \\
\pi_{\text{ALD}}(\boldsymbol{\beta} \mid \theta, \mathbf{y}, \mathbf{X}; \tau) &= \frac{1}{Z_{\text{ALD}}(\theta, \pi)} \exp \left(-\theta \sum_{i=1}^n \rho_{\tau}(e_i(\boldsymbol{\beta})) \right) \pi(\boldsymbol{\beta}),
\end{aligned}$$

where $e_i(\boldsymbol{\beta}) = y_i - \mathbf{x}_i^T \boldsymbol{\beta}$, and Z_{BSQR} and Z_{ALD} are the respective normalizing constants. The ratio of these posteriors is

$$\begin{aligned}
R(\boldsymbol{\beta}) &:= \frac{\pi_{\text{BSQR}}(\boldsymbol{\beta} \mid \theta, h, \mathbf{y}, \mathbf{X}; \tau, h)}{\pi_{\text{ALD}}(\boldsymbol{\beta} \mid \theta, \mathbf{y}, \mathbf{X}; \tau)} = \frac{Z_{\text{ALD}}(\theta, \pi)}{Z_{\text{BSQR}}(\theta, h, \pi)} \cdot \frac{\exp(-\theta \sum_{i=1}^n L_h(e_i(\boldsymbol{\beta}); \tau)) \pi(\boldsymbol{\beta})}{\exp(-\theta \sum_{i=1}^n \rho_{\tau}(e_i(\boldsymbol{\beta}))) \pi(\boldsymbol{\beta})} \\
&= C_0 \cdot \exp \left(-\theta \sum_{i=1}^n [L_h(e_i(\boldsymbol{\beta}); \tau) - \rho_{\tau}(e_i(\boldsymbol{\beta}))] \right),
\end{aligned}$$

where $C_0 = Z_{\text{ALD}}(\theta, \pi) / Z_{\text{BSQR}}(\theta, h, \pi)$ is a positive constant independent of $\boldsymbol{\beta}$. Let $\Delta_i(\boldsymbol{\beta}) = L_h(e_i(\boldsymbol{\beta}); \tau) - \rho_{\tau}(e_i(\boldsymbol{\beta}))$. Without loss of generality, we may re-center $K(v)$ to have zero mean, which implies the symmetry $K(v) = K(-v)$. If the initial compact support is $[a, b]$, this centering implies an effective symmetric support $[-c, c]$ where $c = (b - a)/2 > 0$, with $K(v) = 0$ for $|v| > c$.

Then, from Eq. (6) with a change of variables $u = v/h$, we have $L_h(e; \tau) = \int_{-c}^c \rho_\tau(hu + e)K(u) \, du$.

The derivative of $L_h(e; \tau) - \rho_\tau(e)$ with respect to e is

$$\frac{d}{de} [L_h(e; \tau) - \rho_\tau(e)] = \int_{-c}^c \psi_\tau(hu + e)K(u) \, du - \psi_\tau(e),$$

where $\psi_\tau(x) = \tau - \mathbb{I}(x < 0)$.

We first examine the case where $e > hc$ (equivalently, $e/h > c$). In this regime, for any $u \in [-c, c]$, the argument $hu + e$ satisfies $hu + e > -hc + e > -hc + hc = 0$. Consequently, $\psi_\tau(hu + e) = \tau$. Furthermore, since $e > hc > 0$, we also have $\psi_\tau(e) = \tau$. The derivative of $L_h(e; \tau) - \rho_\tau(e)$ with respect to e is therefore:

$$\frac{d}{de} [L_h(e; \tau) - \rho_\tau(e)] = \int_{-c}^c \tau K(u) \, du - \tau = \tau \int_{-c}^c K(u) \, du - \tau = 0.$$

This implies that $L_h(e; \tau) - \rho_\tau(e)$ remains constant for $e > hc$. To determine this constant value, we directly evaluate the difference:

$$L_h(e; \tau) - \rho_\tau(e) = \int_{-c}^c [\rho_\tau(hu + e) - \rho_\tau(e)]K(u) \, du.$$

Given $e > hc$, both $hu + e$ and e are positive. Hence, $\rho_\tau(x) = \tau x$ for $x > 0$. The integrand simplifies to $\tau(hu + e) - \tau e = \tau hu$. The integral then becomes

$$\int_{-c}^c \tau hu K(u) \, du = \tau h \int_{-c}^c u K(u) \, du = 0,$$

since $\int_{-c}^c u K(u) \, du = 0$ due to $K(u)$ is symmetric about 0 on its support $[-c, c]$. Therefore, for $e > hc$, it follows that $L_h(e; \tau) = \rho_\tau(e)$.

Next, we consider the case where $e < -hc$ (equivalently, $e/h < -c$). In this regime, for any $u \in [-c, c]$, the argument $hu + e$ satisfies $hu + e < hc + e < hc - hc = 0$. Consequently, $\psi_\tau(hu + e) = \tau - 1$. Furthermore, since $e < -hc < 0$, we have $\psi_\tau(e) = \tau - 1$. The derivative of

$L_h(e; \tau) - \rho_\tau(e)$ with respect to e is:

$$\frac{d}{de} [L_h(e; \tau) - \rho_\tau(e)] = \int_{-c}^c (\tau - 1)K(u) du - (\tau - 1) = (\tau - 1) \int_{-c}^c K(u) du - (\tau - 1) = 0.$$

This implies that $L_h(e; \tau) - \rho_\tau(e)$ is also constant for $e < -hc$. To determine this constant, we evaluate the difference:

$$L_h(e; \tau) - \rho_\tau(e) = \int_{-c}^c [\rho_\tau(hu + e) - \rho_\tau(e)]K(u) du.$$

Given $e < -hc$, both $hu + e$ and e are negative. Hence, $\rho_\tau(x) = (\tau - 1)x$ for $x < 0$. The integrand simplifies to $(\tau - 1)(hu + e) - (\tau - 1)e = (\tau - 1)hu$. The integral then becomes

$$\int_{-c}^c (\tau - 1)huK(u) du = (\tau - 1)h \int_{-c}^c uK(u) du = 0.$$

Therefore, for $e < -hc$, it follows that $L_h(e; \tau) = \rho_\tau(e)$.

Based on the previous case analysis, we conclude that for residuals $e_i(\beta)$ satisfying $|e_i(\beta)/h| > c$, $\Delta_i(\beta) = 0$. For residuals $e_i(\beta)$ such that $|e_i(\beta)/h| \leq c$, $e_i(\beta)$ lies in the compact interval $[-hc, hc]$. Within this interval, $L_h(u; \tau)$ and $\rho_\tau(u)$ are continuous functions of u on $[-hc, hc]$. The continuity of $L_h(u; \tau)$ on $[-hc, hc]$ follows from the continuity of $\rho_\tau(u)$ and the properties of convolution with a well-behaved kernel $K(u)$. Thus, $\Delta_i(\beta)$ is also a continuous function of $e_i(\beta)$ over this interval. By the Extreme Value Theorem, there exist constants $m_{\text{in}}(h, \tau, c)$ and $M_{\text{in}}(h, \tau, c)$ such that for all $u \in [-hc, hc]$, $m_{\text{in}}(h, \tau, c) \leq \Delta_i(\beta) \leq M_{\text{in}}(h, \tau, c)$. Let $m_L = \min(0, m_{\text{in}}(h, \tau, c))$ and $M_U = \max(0, M_{\text{in}}(h, \tau, c))$. It follows that $m_L \leq \Delta_i(\beta) \leq M_U$ for any $e_i(\beta)$. Consequently, $\sum_{i=1}^n \Delta_i(\beta)$ is bounded as:

$$n \cdot m_L \leq \sum_{i=1}^n \Delta_i(\beta) \leq n \cdot M_U.$$

The exponential term $\exp(-\theta \sum_{i=1}^n \Delta_i(\beta))$ is therefore bounded below by $\exp(-\theta n M_U)$ and above

by $\exp(-\theta nm_L)$. Thus, the ratio $R(\beta)$ satisfies:

$$C_0 \exp(-\theta n M_U) \leq R(\beta) \leq C_0 \exp(-\theta nm_L).$$

Denoting these lower and upper bounds as $M_1 = C_0 \exp(-\theta n M_U)$ and $M_2 = C_0 \exp(-\theta nm_L)$ respectively, we observe that M_1 and M_2 are positive constants independent of β . This establishes the desired result. \square

Proof of Theorem 5. We evaluate the Hessian $\mathbf{H}_L(\beta; K)$ at the true parameter $\beta_0(\tau)$. At this point, the residuals become the true errors, $e_i(\beta_0(\tau)) = \varepsilon_{0i}$, and from Eq. (14), we have

$$\mathbf{H}_L(\beta_0(\tau); K) = \frac{\theta}{h} \sum_{i=1}^n K\left(\frac{\varepsilon_{0i}}{h}\right) \mathbf{x}_i \mathbf{x}_i^\top.$$

Then, the expected Hessian is

$$\begin{aligned} \mathcal{H}_L(\beta_0(\tau); K) &= \mathbb{E}_{\varepsilon_{0i} \sim f_{\varepsilon_0}, \mathbf{x}_i \sim P_{\mathbf{X}}} \left[\frac{\theta}{h} \sum_{i=1}^n K\left(\frac{\varepsilon_{0i}}{h}\right) \mathbf{x}_i \mathbf{x}_i^\top \right] \\ &= \frac{\theta}{h} \sum_{i=1}^n \mathbb{E}_{\varepsilon_{0i} \sim f_{\varepsilon_0}, \mathbf{x}_i \sim P_{\mathbf{X}}} \left[K\left(\frac{\varepsilon_{0i}}{h}\right) \mathbf{x}_i \mathbf{x}_i^\top \right] \\ &= \frac{\theta}{h} \sum_{i=1}^n s_K(h) \cdot \mathbb{E}[\mathbf{x}_i \mathbf{x}_i^\top] = \frac{\theta}{h} n s_K(h) \Sigma_x \end{aligned}$$

by using the independence of ε_{0i} and \mathbf{x}_i . The relationship between $\mathcal{H}_L(\beta_0(\tau); K_A)$ and $\mathcal{H}_L(\beta_0(\tau); K_B)$ is determined by examining their difference

$$\mathcal{H}_L(\beta_0(\tau); K_A) - \mathcal{H}_L(\beta_0(\tau); K_B) = \frac{\theta}{h} n (s_{K_A}(h) - s_{K_B}(h)) \Sigma_x.$$

The scalar term $c := \frac{\theta}{h} n (s_{K_A}(h) - s_{K_B}(h)) > 0$, since $s_{K_A}(h) - s_{K_B}(h) > 0$ by assumption, and $\theta > 0, h > 0$. Since the matrix Σ_x is positive definite by assumption, the difference is positive definite (strict Loewner order).

For the sample Hessian, the difference is $\theta/h \sum_{i=1}^n (K_A\left(\frac{\varepsilon_{0i}}{h}\right) - K_B\left(\frac{\varepsilon_{0i}}{h}\right)) \mathbf{x}_i \mathbf{x}_i^\top$, which is a sum

of random matrices. By the law of large numbers, the normalized version $1/n(\mathbf{H}_L(\beta_0(\tau); K_A) - \mathbf{H}_L(\beta_0(\tau); K_B)) \xrightarrow{P} \theta/h(s_{K_A}(h) - s_{K_B}(h))\Sigma_x > \mathbf{0}$ as $n \rightarrow \infty$, ensuring the strict inequality holds asymptotically with probability approaching 1. \square

Appendix B: Algorithms

Algorithm 1: Hamiltonian Monte Carlo sampling for β

Input: Data (\mathbf{y}, \mathbf{X}) , current precision value θ_c , quantile level τ , bandwidth h ; prior specification $\pi(\beta)$; initial state $\beta^{(0)}$; number of MCMC iterations N ; HMC leapfrog steps J ; HMC step size ϵ ; HMC mass matrix M .

Output: Markov chain samples $\{\beta^{(1)}, \dots, \beta^{(N)}\}$ approximately from $\pi(\beta | \theta_c, \mathbf{y}, \mathbf{X}; \tau, h)$.

for $k = 1, \dots, N$ **do**

 Let $\beta_c = \beta^{(k-1)}$;

Step 1 (Momentum Sampling):

 Draw an initial momentum $\mathbf{p}_c \sim \mathcal{N}(\mathbf{0}, M)$;

 Set $\tilde{\beta} \leftarrow \beta_c$ and $\tilde{\mathbf{p}} \leftarrow \mathbf{p}_c$;

Step 2 (Trajectory Simulation):

for $l = 1, \dots, L$ **do**

$\mathbf{p}_{\text{half}} \leftarrow \tilde{\mathbf{p}} - (\epsilon/2)\nabla_{\beta}U(\tilde{\beta} | \theta_c, \mathbf{y}, \mathbf{X})$;

$\tilde{\beta} \leftarrow \tilde{\beta} + \epsilon M^{-1} \mathbf{p}_{\text{half}}$;

$\tilde{\mathbf{p}} \leftarrow \mathbf{p}_{\text{half}} - (\epsilon/2)\nabla_{\beta}U(\tilde{\beta} | \theta_c, \mathbf{y}, \mathbf{X})$;

end

 Let the proposal be $(\beta^*, \mathbf{p}^*) = (\tilde{\beta}, \tilde{\mathbf{p}})$;

Step 3 (Metropolis Acceptance):

 Calculate acceptance probability:

$$\alpha = \min \left(1, \frac{\exp(-U(\beta^* | \theta_c, \mathbf{y}, \mathbf{X}) - K(\mathbf{p}^*))}{\exp(-U(\beta_c | \theta_c, \mathbf{y}, \mathbf{X}) - K(\mathbf{p}_c))} \right); \quad (\text{B.1})$$

 Draw $u \sim \text{Uniform}(0, 1)$;

if $u < \alpha$ **then**

 | Set $\beta^{(k)} \leftarrow \beta^*$;

end

else

 | Set $\beta^{(k)} \leftarrow \beta_c$;

end

end

Algorithm 2: Metropolis-Hastings sampling for θ

Input: Data $(\mathbf{y}, \mathcal{X})$, current regression coefficients β_c , quantile level τ , bandwidth h ; prior parameters (a_θ, b_θ) for $\pi(\theta)$; initial state $\theta^{(0)}$; number of MCMC iterations N ; MH proposal variance $\sigma_{\log \theta}^2$.

Output: Markov chain samples $\{\theta^{(1)}, \dots, \theta^{(N)}\}$ approximately from $\pi(\theta | \beta_c, \mathbf{y}, \mathcal{X}; \tau, h)$.

for $k = 1, \dots, N$ **do**

 Let $\theta_c \leftarrow \theta^{(k-1)}$;

 Let $\beta_c \leftarrow \beta^{(k)}$ (from Algorithm 1);

Step 1 (Proposal Generation):

 Generate $z \sim \mathcal{N}(0, 1)$;

 Propose $\theta^* \leftarrow \theta_c \exp(\sigma_{\log \theta} z)$;

Step 2 (Calculate Normalizing Constants):

 Numerically evaluate $Z(\theta_c, \tau, h) = \int_{-\infty}^{\infty} \exp(-\theta_c L_h(u; \tau)) du$;

 Numerically evaluate $Z(\theta^*, \tau, h) = \int_{-\infty}^{\infty} \exp(-\theta^* L_h(u; \tau)) du$;

 ; // Requires numerical integration using the specific $L_h(u; \tau)$ for the chosen kernel.

Step 3 (Metropolis-Hastings Acceptance):

 Calculate $S(\beta_c; \tau, h) \leftarrow \sum_{i=1}^n L_h(y_i - \mathbf{x}_i^\top \beta_c; \tau)$;

 Calculate the log acceptance ratio $\log r$:

$$\begin{aligned} \log r \leftarrow & -(\theta^* - \theta_c)S(\beta_c; \tau, h) - n(\log Z(\theta^*, \tau, h) - \log Z(\theta_c, \tau, h)) \\ & + a_\theta(\log \theta^* - \log \theta_c) - b_\theta(\theta^* - \theta_c); \end{aligned}$$

 Calculate acceptance probability $\alpha \leftarrow \min(1, \exp(\log r))$;

 Draw $u \sim \text{Uniform}(0, 1)$;

if $u < \alpha$ **then**

 | Set $\theta^{(k)} \leftarrow \theta^*$;

end

else

 | Set $\theta^{(k)} \leftarrow \theta_c$;

end

end

Appendix C: Derivations

C.1 Gaussian kernel

The standard Gaussian kernel is $K(v) = \phi(v) = (2\pi)^{-1/2} \exp(-v^2/2)$, with CDF $F_K(u) = \Phi(u)$.

Applying Eq. (16) yields the smoothed score function:

$$\Psi_h(e; \tau) = \Phi\left(\frac{e}{h}\right) - (1 - \tau).$$

The smoothed loss function $L_h(e; \tau)$ is defined such that its derivative is the smoothed score, $L'_h(e; \tau) = \Psi_h(e; \tau)$. We find its form by computing the indefinite integral of $\Psi_h(e; \tau)$ and determining the constant of integration.

$$\begin{aligned} L_h(e; \tau) &= \int \Psi_h(e; \tau) \, de = \int \left(\Phi\left(\frac{e}{h}\right) - (1 - \tau) \right) \, de \\ &= \int \Phi\left(\frac{e}{h}\right) \, de - (1 - \tau)e + C_{G1}. \end{aligned}$$

The first integral, $\int \Phi(e/h) \, de$, is evaluated using integration by parts ($\int u \, dv = uv - \int v \, du$). Let $u = \Phi(e/h)$ and $dv = de$ (so $v = e$), then $du = \frac{1}{h}\phi(e/h) \, de$. This gives:

$$\int \Phi\left(\frac{e}{h}\right) \, de = e\Phi\left(\frac{e}{h}\right) - \int e \cdot \frac{1}{h}\phi\left(\frac{e}{h}\right) \, de.$$

The remaining integral is solved by substitution. Let $w = -e^2/(2h^2)$, then $dw = -e/h^2 \, de$, which implies $e \, de = -h^2 \, dw$. Thus,

$$\begin{aligned} \int e\phi\left(\frac{e}{h}\right) \, de &= \int \frac{1}{\sqrt{2\pi}} e^{-e^2/(2h^2)} e \, de = \frac{1}{\sqrt{2\pi}} \int e^w (-h^2 \, dw) \\ &= -h^2 \frac{1}{\sqrt{2\pi}} \int e^w \, dw = -h^2 \frac{1}{\sqrt{2\pi}} e^w + C_{G2} = -h^2 \phi\left(\frac{e}{h}\right) + C_{G2}. \end{aligned}$$

Substituting this back and combining constants (letting $C_G = C_{G1} - C_{G2}$), we obtain the general form of the smoothed loss:

$$\begin{aligned} L_h(e; \tau) &= e\Phi\left(\frac{e}{h}\right) - \frac{1}{h}\left(-h^2\phi\left(\frac{e}{h}\right)\right) - (1 - \tau)e + C_G \\ &= e\left(\Phi\left(\frac{e}{h}\right) - (1 - \tau)\right) + h\phi\left(\frac{e}{h}\right) + C_G. \end{aligned}$$

The constant of integration C_G is determined by the condition that $L_h(e; \tau) \rightarrow \rho_\tau(e)$ as $h \rightarrow 0$. For any $e > 0$, we require $\lim_{h \rightarrow 0} L_h(e; \tau) = \rho_\tau(e) = e\tau$. As $h \rightarrow 0$, $\Phi(e/h) \rightarrow 1$ and $h\phi(e/h) \rightarrow 0$.

The limit becomes:

$$e(1 - (1 - \tau)) + 0 + C_G = e\tau \implies e\tau + C_G = e\tau,$$

which implies $C_G = 0$. A similar analysis for $e < 0$ also yields $C_G = 0$. Therefore, the smoothed loss function is:

$$L_h(e; \tau) = e\left(\Phi\left(\frac{e}{h}\right) - (1 - \tau)\right) + h\phi\left(\frac{e}{h}\right).$$

This derived form aligns with established results in the literature (e.g., [Horowitz, 1998](#); [Koenker, 2005](#)).

C.2 Uniform kernel

The standard Uniform kernel is defined as $K(v) = 1/2$ for $v \in [-1, 1]$ and $K(v) = 0$ otherwise. Its corresponding CDF, $F_K(u)$, is given by:

$$F_K(u) = \begin{cases} 0 & \text{if } u < -1, \\ \frac{u+1}{2} & \text{if } -1 \leq u \leq 1, \\ 1 & \text{if } u > 1. \end{cases}$$

Substituting this CDF into the general expression for $\Psi_h(e; \tau)$ in Eq. (16), we obtain a piecewise function for $\Psi_h(e; \tau)$ with the Uniform kernel:

$$\Psi_h(e; \tau) = \begin{cases} -(1 - \tau) & \text{if } e/h < -1, \\ \frac{e}{2h} + \tau - \frac{1}{2} & \text{if } -1 \leq e/h \leq 1, \\ \tau & \text{if } e/h > 1. \end{cases}$$

The smoothed loss function $L_h(e; \tau)$ is constructed to match the pinball loss $\rho_\tau(e)$ in the outer regions where $|e/h| \geq 1$. Specifically, $L_h(e; \tau) = e(\tau - 1)$ for $e/h \leq -1$ (i.e., $e \leq -h$), and $L_h(e; \tau) = e\tau$ for $e/h \geq 1$ (i.e., $e \geq h$).

In the central region, where $-1 < e/h < 1$ (i.e., $-h < e < h$), $L_h(e; \tau)$ is obtained by integrating the corresponding segment of $\Psi_h(e; \tau)$:

$$L_h(e; \tau) = \int \left(\frac{e}{2h} + \tau - \frac{1}{2} \right) de = \frac{e^2}{4h} + e \left(\tau - \frac{1}{2} \right) + C_U,$$

where C_U is the constant of integration for this segment. To ensure continuity of $L_h(e; \tau)$ at the boundary $e = -h$, the value of the central segment's expression at $e = -h$ must equal the value from the left segment, which is $\rho_\tau(-h) = (-h)(\tau - 1) = h(1 - \tau)$. Setting these equal allows us to solve for C_U : $(-h)^2/4h + (-h) \left(\tau - \frac{1}{2} \right) + C_U = h(1 - \tau)$, we have $C_U = h/4$. Substituting it into the expression for the central segment, the complete piecewise definition of the smoothed loss function $L_h(e; \tau)$ for the Uniform kernel is:

$$L_h(e; \tau) = \begin{cases} e(\tau - 1) & \text{if } e/h \leq -1, \\ \frac{e^2}{4h} + e \left(\tau - \frac{1}{2} \right) + \frac{h}{4} & \text{if } -1 < e/h < 1, \\ e\tau & \text{if } e/h \geq 1. \end{cases}$$

This construction ensures $L_h(e; \tau)$ is continuous at $e = -h$. We now verify continuity at the other

boundary, $e = h$. For the central segment evaluated at $e = h$, we have

$$L_h(h; \tau) = \frac{h^2}{4h} + h \left(\tau - \frac{1}{2} \right) + \frac{h}{4} = h\tau.$$

This value matches the expression for $L_h(e; \tau)$ in the region $e/h \geq 1$ when $e = h$, i.e., $L_h(h; \tau) = h\tau = \rho_\tau(h)$. Thus, continuity is also satisfied at $e = h$, and the derived $L_h(e; \tau)$ is continuous across all regions.

C.3 Epanechnikov kernel

The standard Epanechnikov kernel is defined by $K(v) = \frac{3}{4}(1 - v^2)$ for $v \in [-1, 1]$ and $K(v) = 0$ otherwise. Its CDF, $F_K(u)$, is piecewise:

$$F_K(u) = \begin{cases} 0 & \text{if } u < -1, \\ \frac{3}{4}u - \frac{1}{4}u^3 + \frac{1}{2} & \text{if } -1 \leq u \leq 1, \\ 1 & \text{if } u > 1. \end{cases}$$

Using this CDF in conjunction with Eq. (16), the expression for $\Psi_h(e; \tau)$ under the Epanechnikov kernel becomes:

$$\Psi_h(e; \tau) = \begin{cases} -(1 - \tau) & \text{if } e/h < -1, \\ \frac{3}{4} \left(\frac{e}{h} \right) - \frac{1}{4} \left(\frac{e}{h} \right)^3 + \tau - \frac{1}{2} & \text{if } -1 \leq e/h \leq 1, \\ \tau & \text{if } e/h > 1. \end{cases}$$

As with other kernels, the smoothed loss function $L_h(e; \tau)$ is designed to replicate the pinball loss $\rho_\tau(e)$ in the regions where $|e/h| \geq 1$. Thus, $L_h(e; \tau) = e(\tau - 1)$ for $e/h \leq -1$, and $L_h(e; \tau) = e\tau$ for $e/h \geq 1$.

For the central region, $-1 < e/h < 1$ (i.e., $-h < e < h$), $L_h(e; \tau)$ is derived by integrating the

relevant segment of $\Psi_h(e; \tau)$:

$$L_h(e; \tau) = \int \left(\frac{3e}{4h} - \frac{e^3}{4h^3} + \tau - \frac{1}{2} \right) de = \frac{3e^2}{8h} - \frac{e^4}{16h^3} + e \left(\tau - \frac{1}{2} \right) + C_E,$$

where C_E is the integration constant for this segment. Continuity at the boundary $e = -h$ dictates that the value of this central expression at $e = -h$ must be equal to $\rho_\tau(-h) = (-h)(\tau - 1) = h(1 - \tau)$. This condition allows for the determination of C_E :

$$\frac{3(-h)^2}{8h} - \frac{(-h)^4}{16h^3} + (-h) \left(\tau - \frac{1}{2} \right) + C_E = h(1 - \tau),$$

which implies that $C_E = 3h/16$. Thus, the complete piecewise definition for $L_h(e; \tau)$ using the Epanechnikov kernel is:

$$L_h(e; \tau) = \begin{cases} e(\tau - 1) & \text{if } e/h \leq -1, \\ \frac{3e^2}{8h} - \frac{e^4}{16h^3} + e \left(\tau - \frac{1}{2} \right) + \frac{3h}{16} & \text{if } -1 < e/h < 1, \\ e\tau & \text{if } e/h \geq 1. \end{cases}$$

This form of $L_h(e; \tau)$ is continuous at $e = -h$ by construction. To confirm overall continuity, we check the boundary $e = h$. Evaluating the central segment at $e = h$:

$$L_h(h; \tau) = \frac{3h^2}{8h} - \frac{h^4}{16h^3} + h \left(\tau - \frac{1}{2} \right) + \frac{3h}{16} = h\tau.$$

This result, $h\tau$, matches the value of $L_h(e; \tau)$ for $e/h \geq 1$ at $e = h$ (i.e., $\rho_\tau(h)$). Therefore, the smoothed loss function $L_h(e; \tau)$ is continuous across all defined regions.

C.4 Triangular kernel

The standard Triangular kernel is given by $K(v) = 1 - |v|$ for $v \in [-1, 1]$ and $K(v) = 0$ otherwise. Its CDF, $F_K(u)$, is defined piecewise:

$$F_K(u) = \begin{cases} 0 & \text{if } u < -1, \\ \frac{1}{2}(1+u)^2 & \text{if } -1 \leq u < 0, \\ 1 - \frac{1}{2}(1-u)^2 & \text{if } 0 \leq u \leq 1, \\ 1 & \text{if } u > 1. \end{cases}$$

Substituting this CDF into Eq. (16), we derive the corresponding $\Psi_h(e; \tau)$:

$$\Psi_h(e; \tau) = \begin{cases} -(1-\tau) & \text{if } e/h < -1, \\ \frac{1}{2} \left(1 + \frac{e}{h}\right)^2 - (1-\tau) & \text{if } -1 \leq e/h < 0, \\ \tau - \frac{1}{2} \left(1 - \frac{e}{h}\right)^2 & \text{if } 0 \leq e/h \leq 1, \\ \tau & \text{if } e/h > 1. \end{cases} \quad (\text{C.1})$$

The smoothed loss function $L_h(e; \tau)$ is constructed to match the pinball loss $\rho_\tau(e)$ in the outer regions where $|e/h| \geq 1$. Thus, $L_h(e; \tau) = e(\tau - 1)$ for $e/h \leq -1$, and $L_h(e; \tau) = e\tau$ for $e/h \geq 1$.

Due to the piecewise nature of $F_K(u)$ for the Triangular kernel around $u = 0$, the central region for $L_h(e; \tau)$ ($-h < e < h$) is split into two segments. For the segment $-1 < e/h < 0$ (i.e., $-h < e < 0$), integrating the corresponding part of $\Psi_h(e; \tau)$ yields:

$$L_h(e; \tau) = \int \left(\frac{1}{2} \left(1 + \frac{e}{h}\right)^2 - (1-\tau) \right) de = \frac{h}{6} \left(1 + \frac{e}{h}\right)^3 - e(1-\tau) + C_{T1}.$$

The constant C_{T1} is determined by ensuring continuity with $\rho_\tau(e)$ at $e = -h$. Setting $L_h(-h; \tau) =$

$\rho_\tau(-h) = h(1 - \tau)$ results in $C_{T1} = 0$. Thus, for $-1 < e/h < 0$:

$$L_h(e; \tau) = \frac{h}{6} \left(1 + \frac{e}{h}\right)^3 - e(1 - \tau).$$

For the segment $0 \leq e/h < 1$ (i.e., $0 \leq e < h$), integration gives:

$$L_h(e; \tau) = \int \left(\tau - \frac{1}{2} \left(1 - \frac{e}{h}\right)^2\right) de = e\tau + \frac{h}{6} \left(1 - \frac{e}{h}\right)^3 + C_{T2}.$$

Similarly, C_{T2} is found by imposing continuity with $\rho_\tau(e)$ at $e = h$. The condition $L_h(h; \tau) = \rho_\tau(h) = h\tau$ yields $C_{T2} = 0$. Thus, for $0 \leq e/h < 1$:

$$L_h(e; \tau) = e\tau + \frac{h}{6} \left(1 - \frac{e}{h}\right)^3.$$

With $C_{T1} = 0$ and $C_{T2} = 0$, we must verify the continuity of $L_h(e; \tau)$ at the internal boundary $e = 0$: (1) As $e/h \rightarrow 0^-$, $L_h(0; \tau) = \frac{h}{6}(1 + 0)^3 - 0 \cdot (1 - \tau) = h/6$; (2) As $e/h \rightarrow 0^+$, $L_h(0; \tau) = 0 \cdot \tau + \frac{h}{6}(1 - 0)^3 = h/6$. Since the limits from both sides are equal, $L_h(e; \tau)$ is continuous at $e = 0$. Combining all segments, the complete expression for $L_h(e; \tau)$ with the Triangular kernel is:

$$L_h(e; \tau) = \begin{cases} e(\tau - 1) & \text{if } e/h \leq -1, \\ \frac{h}{6} \left(1 + \frac{e}{h}\right)^3 - e(1 - \tau) & \text{if } -1 < e/h < 0, \\ e\tau + \frac{h}{6} \left(1 - \frac{e}{h}\right)^3 & \text{if } 0 \leq e/h < 1, \\ e\tau & \text{if } e/h \geq 1. \end{cases}$$

This smoothed loss function $L_h(e; \tau)$ is continuous across all regions. Furthermore, owing to the continuity of the Triangular kernel $K(v)$ itself, the derivative function $\Psi_h(e; \tau)$ given in Eq. (C.1) is also continuous for all e .

Appendix D: Simulation results

Table D. Full simulation results comparing StdQR, BQR-ALD, and our proposed BSQR with Gaussian (G), Uniform (U), Epanechnikov (E), and Triangular (T) kernels.

Error Dist.	Design	τ	Method	Estimation Accuracy (β)			Prediction		Inference (β)		Computation		MCMC Diag. (β)	
				MSE	MAE	WMSE	Check Loss	Coverage	CI Width	Time (s)	\hat{R}_{\max}	ESS _{min}		
$\mathcal{N}(0, 1)$	Sparse ($p = 20$)	0.25	StdQR	0.0179	0.1072	0.2186	0.4398	—	—	—	—	—	—	—
		0.25	BQR-ALD	0.0157	0.1005	0.1928	0.7478	0.8692	0.3748	25.82	1.0021	2333.4		
		0.25	BSQR-G	0.0161	0.1008	0.2061	0.4374	0.8765	0.8954	130.18	1.0060	3113.7		
		0.25	BSQR-U	0.0154	0.0996	0.1900	0.4353	0.8715	0.3757	6.47	1.0019	2985.3		
		0.25	BSQR-E	0.0155	0.0996	0.1901	0.4353	0.9295	0.4566	39.39	1.0020	2928.4		
		0.25	BSQR-T	0.0155	0.0998	0.1905	0.4353	0.8732	0.3743	30.92	1.0019	2904.1		
	Full	0.50	StdQR	0.0143	0.0950	0.1729	0.4322	—	—	—	—	—	—	—
		0.50	BQR-ALD	0.0115	0.0859	0.1404	0.4265	0.9205	0.3773	27.64	1.0021	2326.5		
		0.50	BSQR-G	0.0109	0.0817	0.1399	0.4254	0.9350	0.8896	129.38	1.0060	3258.2		
		0.50	BSQR-U	0.0107	0.0829	0.1307	0.4246	0.9300	0.3713	6.45	1.0019	3111.8		
		0.50	BSQR-E	0.0105	0.0822	0.1286	0.4242	0.9855	0.5510	37.72	1.0019	3034.8		
		0.50	BSQR-T	0.0110	0.0841	0.1348	0.4253	0.9258	0.3734	30.65	1.0019	3006.9		
	Large	0.75	StdQR	0.0181	0.1065	0.2233	0.4424	—	—	—	—	—	—	—
		0.75	BQR-ALD	0.0154	0.0989	0.1909	0.7496	0.8652	0.3763	26.25	1.0021	2339.5		

Continued on next page

Table D. – *Continued from previous page*

Error Dist.	Design	τ	Method	Estimation Accuracy (β)			Prediction		Inference (β)		Computation		MCMC Diag. (β)	
				MSE	MAE	WMSE	Check Loss	Coverage	CI Width	Time (s)	\hat{R}_{\max}	ESS _{min}		
0.75	BSQR	0.75	BSQR-G	0.0166	0.0998	0.2239	0.4399	0.8782	0.8964	125.60	1.0060	3104.5		
		0.75	BSQR-U	0.0151	0.0979	0.1874	0.4360	0.8712	0.3775	6.38	1.0020	3022.6		
		0.75	BSQR-E	0.0151	0.0981	0.1878	0.4361	0.9305	0.4503	39.69	1.0019	2963.9		
		0.75	BSQR-T	0.0152	0.0982	0.1881	0.4362	0.8675	0.3759	31.28	1.0019	2946.9		
Dense ($p = 8$)	BSQR	0.25	StdQR	0.0159	0.1005	0.0808	0.4145	—	—	—	—	—	—	—
		0.25	BQR-ALD	0.0142	0.0951	0.0725	0.7915	0.8625	0.3570	10.08	1.0018	2174.8		
		0.25	BSQR-G	0.0136	0.0933	0.0699	0.4127	0.8850	0.3665	85.94	1.0015	2804.2		
		0.25	BSQR-U	0.0137	0.0932	0.0698	0.4126	0.8694	0.3558	4.27	1.0016	2734.7		
		0.25	BSQR-E	0.0136	0.0929	0.0697	0.4126	0.9362	0.4378	25.87	1.0015	2722.6		
		0.25	BSQR-T	0.0138	0.0935	0.0705	0.4127	0.8638	0.3554	20.39	1.0017	2705.3		
0.50	BSQR	0.50	StdQR	0.0129	0.0902	0.0651	0.4108	—	—	—	—	—	—	—
		0.50	BQR-ALD	0.0109	0.0825	0.0555	0.4092	0.9088	0.3568	10.09	1.0018	2186.0		
		0.50	BSQR-G	0.0111	0.0776	0.0804	0.4110	0.9269	0.8671	88.83	1.0058	2842.0		
		0.50	BSQR-U	0.0098	0.0779	0.0501	0.4081	0.9150	0.3514	4.28	1.0016	2751.5		
		0.50	BSQR-E	0.0099	0.0781	0.0502	0.4081	0.9800	0.5039	24.98	1.0016	2722.8		
		0.50	BSQR-T	0.0102	0.0795	0.0520	0.4085	0.9138	0.3534	20.30	1.0017	2732.6		
0.75	BSQR	0.75	StdQR	0.0167	0.1032	0.0850	0.4156	—	—	—	—	—	—	—

Table D. – *Continued from previous page*

Error Dist.	Design	τ	Method	Estimation Accuracy (β)			Prediction		Inference (β)		Computation		MCMC Diag. (β)	
				MSE	MAE	WMSE	Check Loss	Coverage	CI Width	Time (s)	\hat{R}_{\max}	ESS_{\min}		
$t(3)$	Sparse ($p = 20$)	0.75	BQR-ALD	0.0152	0.0980	0.0769	0.7913	0.8494	0.3585	10.03	1.0018	2164.1		
		0.75	BSQR-G	0.0147	0.0969	0.0747	0.4135	0.8700	0.3660	84.97	1.0016	2822.5		
		0.75	BSQR-U	0.0145	0.0963	0.0737	0.4133	0.8588	0.3575	4.30	1.0017	2777.2		
		0.75	BSQR-E	0.0146	0.0963	0.0740	0.4134	0.9138	0.4276	25.69	1.0016	2730.7		
		0.75	BSQR-T	0.0146	0.0966	0.0743	0.4135	0.8525	0.3565	20.39	1.0016	2729.3		
\mathcal{G}_2	Sparse ($p = 20$)	0.25	StdQR	0.0238	0.1228	0.2905	0.6021	—	—	—	—	—	—	—
		0.25	BQR-ALD	0.0212	0.1159	0.2601	1.0805	0.9022	0.4859	23.25	1.0021	2347.4		
		0.25	BSQR-G	0.0215	0.1169	0.2657	0.5982	0.9118	0.5085	115.82	1.0019	3043.3		
		0.25	BSQR-U	0.0215	0.1167	0.2642	0.5979	0.9058	0.4929	6.29	1.0020	2938.7		
		0.25	BSQR-E	0.0214	0.1166	0.2640	0.5979	0.9432	0.5650	39.01	1.0020	2905.6		
		0.25	BSQR-T	0.0213	0.1162	0.2618	0.5975	0.9048	0.4897	30.24	1.0019	2907.8		
\mathcal{G}_2	Sparse ($p = 20$)	0.50	StdQR	0.0190	0.1096	0.2326	0.5905	—	—	—	—	—	—	—
		0.50	BQR-ALD	0.0156	0.0995	0.1910	0.5837	0.9468	0.4874	23.64	1.0022	2363.2		
		0.50	BSQR-G	0.0153	0.0987	0.1889	0.5832	0.9570	0.5026	115.96	1.0019	3169.1		
		0.50	BSQR-U	0.0154	0.0987	0.1887	0.5832	0.9530	0.4960	6.35	1.0020	3112.6		
		0.50	BSQR-E	0.0153	0.0984	0.1881	0.5831	0.9915	0.7114	38.36	1.0019	3058.0		
		0.50	BSQR-T	0.0154	0.0987	0.1886	0.5832	0.9502	0.4912	29.51	1.0020	2996.5		

Continued on next page

Table D. – *Continued from previous page*

Error Dist.	Design	τ	Method	Estimation Accuracy (β)			Prediction		Inference (β)		Computation		MCMC Diag. (β)	
				MSE	MAE	WMSE	Check Loss	Coverage	CI Width	Time (s)	\hat{R}_{\max}	ESS_{\min}		
ω	Dense ($p = 8$)	0.75	StdQR	0.0241	0.1230	0.2940	0.5991	—	—	—	—	—	—	—
		0.75	BQR-ALD	0.0221	0.1176	0.2690	1.0923	0.9030	0.4929	23.40	1.0020	2332.6		
		0.75	BSQR-G	0.0241	0.1210	0.3165	0.6003	0.9112	1.0306	119.20	1.0059	3031.9		
		0.75	BSQR-U	0.0225	0.1186	0.2741	0.5961	0.9008	0.4995	6.33	1.0019	2925.5		
		0.75	BSQR-E	0.0225	0.1184	0.2736	0.5960	0.9410	0.5708	39.56	1.0019	2910.4		
		0.75	BSQR-T	0.0223	0.1181	0.2713	0.5957	0.9010	0.4966	30.47	1.0019	2907.0		
ω	Dense ($p = 8$)	0.25	StdQR	0.0194	0.1121	0.1018	0.5687	—	—	—	—	—	—	—
		0.25	BQR-ALD	0.0176	0.1067	0.0919	1.1289	0.9006	0.4436	9.79	1.0017	2225.9		
		0.25	BSQR-G	0.0181	0.1084	0.0937	0.5672	0.9106	0.4677	79.16	1.0016	2779.1		
		0.25	BSQR-U	0.0180	0.1082	0.0931	0.5672	0.9050	0.4535	4.16	1.0015	2735.0		
		0.25	BSQR-E	0.0179	0.1078	0.0926	0.5671	0.9525	0.5490	24.63	1.0016	2701.2		
		0.25	BSQR-T	0.0177	0.1074	0.0919	0.5669	0.9025	0.4488	21.69	1.0070	2705.1		
ω	Dense ($p = 8$)	0.50	StdQR	0.0149	0.0969	0.0756	0.5651	—	—	—	—	—	—	—
		0.50	BQR-ALD	0.0129	0.0907	0.0657	0.5635	0.9488	0.4418	10.04	1.0017	2248.7		
		0.50	BSQR-G	0.0126	0.0900	0.0637	0.5632	0.9556	0.4612	77.73	1.0015	2811.1		
		0.50	BSQR-U	0.0126	0.0897	0.0639	0.5632	0.9550	0.4526	4.29	1.0016	2757.1		
		0.50	BSQR-E	0.0125	0.0896	0.0634	0.5632	0.9931	0.6434	24.30	1.0016	2753.5		

Continued on next page

Table D. – *Continued from previous page*

Error Dist.	Design	τ	Method	Estimation Accuracy (β)			Prediction		Inference (β)		Computation		MCMC Diag. (β)	
				MSE	MAE	WMSE	Check Loss	Coverage	CI Width	Time (s)	\hat{R}_{\max}	ESS_{\min}		
0.2 $\mathcal{N}(0, 3)$ +0.8 $\mathcal{N}(0, 4)$	Sparse ($p = 20$)	0.50	BSQR-T	0.0127	0.0900	0.0644	0.5633	0.9531	0.4466	19.91	1.0015	2734.2		
		0.75	StdQR	0.0193	0.1093	0.0956	0.5660	—	—	—	—	—	—	
		0.75	BQR-ALD	0.0182	0.1052	0.0894	1.1368	0.9069	0.4495	9.77	1.0017	2221.7		
		0.75	BSQR-G	0.0188	0.1065	0.0924	0.5655	0.9181	0.4746	78.23	1.0015	2797.0		
		0.75	BSQR-U	0.0186	0.1060	0.0912	0.5653	0.9088	0.4597	4.20	1.0016	2757.2		
		0.75	BSQR-E	0.0184	0.1057	0.0908	0.5652	0.9475	0.5398	24.79	1.0016	2734.1		
		0.75	BSQR-T	0.0183	0.1053	0.0901	0.5651	0.9088	0.4541	19.84	1.0015	2686.3		
0.2 $\mathcal{N}(0, 3)$ +0.8 $\mathcal{N}(0, 4)$	Full ($p = 100$)	0.25	StdQR	0.0697	0.2130	0.8426	0.8584	—	—	—	—	—	—	
		0.25	BQR-ALD	0.0611	0.1987	0.7334	1.4624	0.8622	0.7370	25.16	1.0021	2310.5		
		0.25	BSQR-G	0.0617	0.1982	0.7641	0.8500	0.8788	1.2841	108.02	1.0060	3002.9		
		0.25	BSQR-U	0.0600	0.1965	0.7191	0.8468	0.8650	0.7391	6.25	1.0020	2985.0		
		0.25	BSQR-E	0.0601	0.1968	0.7209	0.8470	0.9288	0.9021	38.29	1.0019	2872.8		
		0.25	BSQR-T	0.0603	0.1971	0.7233	0.8472	0.8645	0.7367	29.84	1.0020	2831.8		
		0.50	StdQR	0.0528	0.1841	0.6408	0.8402	—	—	—	—	—	—	
0.2 $\mathcal{N}(0, 3)$ +0.8 $\mathcal{N}(0, 4)$	Sparse ($p = 20$)	0.50	BQR-ALD	0.0426	0.1654	0.5161	0.8280	0.9295	0.7383	25.10	1.0022	2305.9		
		0.50	BSQR-G	0.0373	0.1548	0.4516	0.8217	0.9418	0.7268	104.16	1.0019	3201.8		
		0.50	BSQR-U	0.0394	0.1590	0.4763	0.8240	0.9342	0.7276	6.23	1.0020	3054.5		

Continued on next page

Table D. – *Continued from previous page*

Error Dist.	Design	τ	Method	Estimation Accuracy (β)			Prediction		Inference (β)		Computation		MCMC Diag. (β)	
				MSE	MAE	WMSE	Check Loss	Coverage	CI Width	Time (s)	\hat{R}_{\max}	ESS_{\min}		
Q	0.50	0.50	BSQR-E	0.0387	0.1577	0.4691	0.8233	0.9912	1.0776	37.75	1.0019	3008.8		
		0.50	BSQR-T	0.0409	0.1621	0.4946	0.8257	0.9318	0.7318	29.59	1.0019	2938.1		
	0.75	0.75	StdQR	0.0696	0.2102	0.8306	0.8542	—	—	—	—	—	—	—
		0.75	BQR-ALD	0.0591	0.1946	0.7104	1.4533	0.8660	0.7298	25.00	1.0022	2326.3		
		0.75	BSQR-G	0.0590	0.1946	0.7101	0.8432	0.8858	0.7632	107.22	1.0020	3061.8		
		0.75	BSQR-U	0.0584	0.1937	0.7016	0.8425	0.8705	0.7327	6.27	1.0019	2953.9		
		0.75	BSQR-E	0.0585	0.1938	0.7031	0.8426	0.9302	0.8741	38.83	1.0019	2895.6		
		0.75	BSQR-T	0.0585	0.1937	0.7026	0.8426	0.8712	0.7302	29.77	1.0019	2872.8		
	Dense ($p = 8$)	0.25	StdQR	0.0632	0.1993	0.3103	0.8032	—	—	—	—	—	—	—
		0.25	BQR-ALD	0.0572	0.1902	0.2807	1.5346	0.8562	0.6967	10.48	1.0019	2168.1		
		0.25	BSQR-G	0.0547	0.1854	0.2725	0.7997	0.8781	0.7278	68.93	1.0015	2767.7		
		0.25	BSQR-U	0.0545	0.1851	0.2706	0.7995	0.8675	0.6971	4.08	1.0017	2714.3		
		0.25	BSQR-E	0.0548	0.1856	0.2713	0.7995	0.9206	0.8624	24.22	1.0016	2720.2		
		0.25	BSQR-T	0.0552	0.1865	0.2726	0.7997	0.8569	0.6937	19.06	1.0015	2650.1		
Q	0.50	0.50	StdQR	0.0479	0.1730	0.2431	0.8006	—	—	—	—	—	—	—
		0.50	BQR-ALD	0.0411	0.1610	0.2075	0.7972	0.9125	0.6870	10.46	1.0017	2158.1		
		0.50	BSQR-G	0.0356	0.1502	0.1798	0.7945	0.9319	0.6785	70.28	1.0015	2788.8		

Continued on next page

Table D. – *Continued from previous page*

Error Dist.	Design	τ	Method	Estimation Accuracy (β)			Prediction		Inference (β)		Computation		MCMC Diag. (β)	
				MSE	MAE	WMSE	Check Loss	Coverage	CI Width	Time (s)	\hat{R}_{\max}	ESS_{\min}		
9	$\mathcal{N}(0, \sigma_i^2)$, $\sigma_i = \exp(-0.25 + 0.5x_{i1})$	0.50	BSQR-U	0.0376	0.1542	0.1905	0.7955	0.9238	0.6762	4.09	1.0015	2755.2		
			BSQR-E	0.0377	0.1543	0.1904	0.7955	0.9812	0.9773	23.71	1.0016	2736.7		
			BSQR-T	0.0390	0.1569	0.1971	0.7961	0.9150	0.6789	19.10	1.0015	2717.1		
		0.75	StdQR	0.0608	0.1966	0.3079	0.8060	—	—	—	—	—	—	
			BQR-ALD	0.0538	0.1841	0.2737	1.5343	0.8538	0.6905	10.30	1.0018	2164.7		
			BSQR-G	0.0520	0.1807	0.2634	0.8020	0.8825	0.7180	68.42	1.0016	2756.3		
		0.75	BSQR-U	0.0519	0.1808	0.2620	0.8018	0.8650	0.6886	4.05	1.0017	2727.4		
			BSQR-E	0.0519	0.1805	0.2631	0.8019	0.9150	0.8209	23.91	1.0016	2716.6		
			BSQR-T	0.0523	0.1813	0.2658	0.8021	0.8612	0.6874	18.66	1.0015	2684.5		
		Sparse ($p = 20$)	0.25	StdQR	0.0096	0.0779	0.1177	0.3824	—	—	—	—	—	—
			BQR-ALD	0.0089	0.0749	0.1091	0.6951	0.9190	0.3203	23.56	1.0020	2345.5		
			BSQR-G	0.0091	0.0759	0.1124	0.3813	0.9178	0.3294	131.95	1.0019	2997.0		
			BSQR-U	0.0091	0.0756	0.1117	0.3811	0.9145	0.3237	6.50	1.0019	2864.6		
			BSQR-E	0.0091	0.0755	0.1115	0.3811	0.9508	0.3696	40.88	1.0020	2843.0		
			BSQR-T	0.0090	0.0754	0.1108	0.3809	0.9145	0.3221	32.05	1.0020	2834.2		
		0.50	StdQR	0.0075	0.0689	0.0932	0.3760	—	—	—	—	—	—	
			BQR-ALD	0.0064	0.0637	0.0800	0.3727	0.9502	0.3133	23.57	1.0021	2313.6		

Continued on next page

Table D. – *Continued from previous page*

Error Dist.	Design	τ	Method	Estimation Accuracy (β)			Prediction		Inference (β)		Computation		MCMC Diag. (β)	
				MSE	MAE	WMSE	Check Loss	Coverage	CI Width	Time (s)	\hat{R}_{\max}	ESS_{\min}		
67	0.50	0.50	BSQR-G	0.0076	0.0654	0.1130	0.3768	0.9538	0.8367	134.71	1.0060	3120.5		
		0.50	BSQR-U	0.0064	0.0636	0.0801	0.3728	0.9515	0.3169	6.52	1.0019	3050.4		
		0.50	BSQR-E	0.0064	0.0636	0.0801	0.3728	0.9915	0.4408	38.72	1.0019	3007.1		
		0.50	BSQR-T	0.0064	0.0634	0.0795	0.3726	0.9512	0.3148	33.26	1.0020	2946.8		
	0.75	0.75	StdQR	0.0100	0.0798	0.1220	0.3823	—	—	—	—	—	—	—
		0.75	BQR-ALD	0.0091	0.0760	0.1113	0.6893	0.9062	0.3151	23.38	1.0021	2332.7		
		0.75	BSQR-G	0.0092	0.0766	0.1136	0.3804	0.9095	0.3243	133.81	1.0020	3007.0		
		0.75	BSQR-U	0.0092	0.0764	0.1129	0.3802	0.9050	0.3187	6.43	1.0020	2906.1		
		0.75	BSQR-E	0.0092	0.0764	0.1131	0.3803	0.9405	0.3598	39.83	1.0019	2815.8		
		0.75	BSQR-T	0.0091	0.0762	0.1123	0.3801	0.9062	0.3173	31.65	1.0019	2837.4		
68	Dense ($p = 8$)	0.25	StdQR	0.0086	0.0728	0.0440	0.3655	—	—	—	—	—	—	—
		0.25	BQR-ALD	0.0081	0.0704	0.0417	0.7278	0.8838	0.2887	9.76	1.0017	2221.1		
		0.25	BSQR-G	0.0104	0.0739	0.0732	0.3685	0.8900	0.8085	92.17	1.0057	2805.3		
		0.25	BSQR-U	0.0083	0.0710	0.0427	0.3652	0.8906	0.2939	4.33	1.0017	2759.1		
		0.25	BSQR-E	0.0083	0.0709	0.0426	0.3652	0.9331	0.3454	26.41	1.0017	2729.9		
		0.25	BSQR-T	0.0082	0.0705	0.0421	0.3651	0.8888	0.2912	20.92	1.0016	2744.6		
		0.50	StdQR	0.0065	0.0649	0.0338	0.3613	—	—	—	—	—	—	—

Continued on next page

Table D. – *Continued from previous page*

Error Dist.	Design	τ	Method	Estimation Accuracy (β)			Prediction		Inference (β)		Computation		MCMC Diag. (β)	
				MSE	MAE	WMSE	Check Loss	Coverage	CI Width	Time (s)	\hat{R}_{\max}	ESS_{\min}		
∞	0.50	0.50	BQR-ALD	0.0057	0.0605	0.0299	0.3602	0.9419	0.2861	9.76	1.0018	2251.1		
		0.50	BSQR-G	0.0055	0.0593	0.0288	0.3600	0.9544	0.2960	95.94	1.0015	2842.0		
		0.50	BSQR-U	0.0055	0.0595	0.0289	0.3600	0.9500	0.2903	4.40	1.0016	2788.6		
		0.50	BSQR-E	0.0055	0.0595	0.0289	0.3600	0.9894	0.3952	25.76	1.0015	2756.1		
		0.50	BSQR-T	0.0055	0.0595	0.0288	0.3599	0.9450	0.2883	24.58	1.0016	2776.2		
∞	0.75	0.75	StdQR	0.0083	0.0725	0.0417	0.3618	—	—	—	—	—	—	—
		0.75	BQR-ALD	0.0073	0.0683	0.0373	0.7194	0.9062	0.2865	9.65	1.0018	2228.6		
		0.75	BSQR-G	0.0076	0.0695	0.0385	0.3610	0.9106	0.2969	91.77	1.0015	2801.1		
		0.75	BSQR-U	0.0076	0.0693	0.0384	0.3610	0.9075	0.2913	4.33	1.0016	2764.9		
		0.75	BSQR-E	0.0075	0.0692	0.0383	0.3609	0.9431	0.3373	25.99	1.0017	2729.0		
		0.75	BSQR-T	0.0074	0.0687	0.0378	0.3608	0.9081	0.2891	25.52	1.0015	2726.5		

Note: **Bold** values indicate superior performance among the Bayesian methods (BQR-ALD and BSQR variants) for key metrics (lower is better for MSE, MAE, WMSE, check loss, CI width, time; for coverage, closer to 0.95 is better; for \hat{R}_{\max} , closer to 1.0 is better; for ESS_{\min} , higher is better). The MCMC diagnostics reported are the maximum potential scale reduction factor (\hat{R}_{\max}) and the minimum bulk effective sample size (ESS_{\min}) across all β coefficients. For our BSQR methods, the average number of divergent transitions per replication was low (consistently below 2) and did not appear to compromise the posterior estimates.